BACKSCATTERING OF ELECTROMAGNETIC WAVE FROM UNDERDENSE TURBULENT PLASMA

Yu-Yun Kuo
(Ph. D. Thesis)

September 23, 1971

AEC Contract No. W-7405-eng-48

DISCLAIMER

BACKSCATTERING OF ELECTROMAGNETIC WAVE

FROM UNDERDENSE TURBULENT PLASMA

Contents

Abstract 1

1. Introduction 3

2. Transport Equation 5

3. Correlation Function for Turbulent Medium 13

4. Solution of Vector Transport Equation 17

4.1. Discrete Coordinate Method 17

4.2. Boundary Conditions 24

5. Backscattering from Slab Geometry 26

5.1. Modification of Transport Equation 26

5.2. Representation of Correlation Function 28

5.3. General Feature of the Scattered Signal 31

6. Application to Ionospheric Aurora 37

7. Born Approximation Controversy Near Critical Density . . . 44

Acknowledgments 46

Footnotes and References 47

Tables 51

Figure Captions 54

Figures 56

LBL-41

BACKSCATTERING OF ELECTROMAGNETIC WAVE FROM UNDERDENSE TURBULENT PLASMA*

Yu-Yun Kuo

Lawrence Berkeley Laboratory
University of California
Berkeley, California 94720

September 23, 1971

ABSTRACT

Backscattering of electromagnetic waves from a homogeneous underdense turbulent slab plasma was studied in a transport approximation of the multiple scattering regime. The general feature of the multiple scattered signal is quite different from that predicted by the Born approximation. There are two parameters which characterize the properties of the scattered signal. One is L_s, the ratio of the slab thickness to the scattering mean free path. The other is ξ, the ratio of the scattering loss to the collisional absorption. When $L_s \ll 1$, the cross section of the parallel polarization $\sigma_{||}$ obtained in the multiple scattering regime remains the same as that gained from Born approximation. But in the region of $L_s \gtrsim 1$, the cross section $\sigma_{||}$ in multiple scattering will level off while that in the Born approximation goes up as a linear function of L_s. The cross section of the cross polarization $\sigma_{\perp}$ of a backward scattered signal has the same feature as $\sigma_{||}$, whereas $\sigma_{\perp}$ in the Born approximation is zero. The absolute magnitude of $\sigma_{||}$, and the relative ratio between $\sigma_{||}$ and $\sigma_{\perp}$ all depend on the parameter ξ.

The calculation was applied to the ionospheric auroral phenomena. It was also found that the criteria for applying the Born approximation up to the critical density does not depend upon the electron density in the medium, but upon the parameter L_s.

1. INTRODUCTION

In the literature, the problem of bistatic scattering and backscattering of electromagnetic waves from plasmas is usually dealt with by means of the first Born approximation,[1] which assumes (1) the incident wave at each point of the scattering medium is the same, and (2) only single scattering needs to be considered. The interference effect of the waves scattered from different point sources is taken care of by the two-particle correlation function σ_g that the total cross section σ depends on σ_g as

$$\sigma(k) \propto \rho^2 \sigma_g(k) ,$$

where k is the wave-vector difference between the incident wave and the scattered wave, and ρ is the density of the scattering source. It is quite obvious that when there is attenuation in the medium due to, for instance, collision loss, or when the scattering mean free path is small compared with the size of the medium, the first Born approximation is not applicable.

Ruffine and de Wolf[2] discussed the problem in the second Born approximation and estimated the cross-polarized scattered power for cylindrical and spherical underdense plasmas. Calculations of higher orders are quite difficult.

The other traditional approach is the phenomenological transport equation.[3] The scalar transport equation has been solved by the iteration method to the second order.[4] The cross-polarization scattering cross section found in this way needs to be justified.

K. M. Watson[5-7] bridged the two approaches by starting from individual electron scattering to arrive at a vector transport equation in the collective multiple-scattering scheme. The two polarizations of each wave were represented by a Stokes column vector.[8] When the transport equation is solved, the scattering power of the parallel polarization, and that of the cross polarization were found automatically.

In this work we will state Watson's approach and the important assumption in the model very briefly in the first chapter. The correlation function, which is the relevant part in the transport equation, will be encountered in Chapter 2. The next chapter explains the method which we have used to solve the vector transport equation. Application of multiple scattering to slab geometry and the problem of the ionospheric aurora are dealt with in Chapters 5 and 6. Finally, we will discuss the question raised recently about the validity of Born approximations near the critical density.

2. TRANSPORT EQUATION[9]

In the multiple scattering regime, the electric field at a point $\underset{\sim}{Z}_\alpha$ will be the sum of the incident field plus the field of the waves scattered from all the electrons. We can write this fundamental relation as the following:

$$\underset{\sim}{E}(\alpha) = \underset{\sim}{E}_I(\alpha) + \sum_{\beta(\neq\alpha)=1}^{N} \sum_{j=1}^{2} \hat{e}_{\alpha\beta}(j)\, E_{\alpha\beta}(\alpha,j) \,, \tag{1}$$

where $\underset{\sim}{E}_I(\alpha) = \hat{e}(1)\, E_0\, \mathrm{Exp}(i\underset{\sim}{k}_{in}\cdot\underset{\sim}{Z}_\alpha)$ is the incident field with polarization $\hat{e}(1)$. The unit vectors $\hat{e}_{\alpha\beta}(1)$ and $\hat{e}_{\alpha\beta}(2)$ are defined by choosing $\hat{z}$ in the z-direction so that

$$\hat{e}_{\alpha\beta}(2) = \frac{\hat{p}_{\alpha\beta} \times \hat{z}}{|\hat{p}_{\alpha\beta} \times \hat{z}|} \tag{2}$$

$$\hat{e}_{\alpha\beta}(1) = \hat{e}_{\alpha\beta}(2) \times \hat{p}_{\alpha\beta} \,,$$

where

$$\hat{p}_{\alpha\beta} = \frac{\underset{\sim}{z}_\alpha - \underset{\sim}{z}_\beta}{|\underset{\sim}{z}_\alpha - \underset{\sim}{z}_\beta|} \,.$$

The quantity $E_{\alpha\beta}(\alpha,j)$ represents the component along $\hat{e}_{\alpha\beta}(j)$ of the electric field of that wave scattered from an electron at $\underset{\sim}{z}_\beta$ to the point $\underset{\sim}{z}_\alpha$. It satisfies the following relation

$$E_{\alpha\beta}(\alpha,i) = G_{\alpha\beta}{}^0\, f_{il}(\alpha\beta,\beta 0)\, E_I(\beta)$$

$$+ \sum_{\sigma(\neq\beta)=1}^{N} \sum_{j=1}^{2} G_{\alpha\beta}{}^0\, f_{ij}(\alpha\beta,\beta\sigma)\, E_{\beta\sigma}(\beta,j) \,, \tag{3}$$

where

$$G_{\alpha\beta}{}^0 = \frac{e^{ik_{in}R_{\alpha\beta}}}{R_{\alpha\beta}} \quad \text{with} \quad R_{\alpha\beta} = |\underset{\sim}{z}_\alpha - \underset{\sim}{z}_\beta|$$

and

$$f_{ij}(\alpha\beta,\beta\sigma) = f_0\, \hat{e}_{\alpha\beta}(i)\cdot\hat{e}_{\beta\sigma}(j) \tag{4}$$

with

$$f_0 = -\frac{e^2}{mc^2} \,.$$

In the above, $f_{ij}(\alpha\beta,\beta\sigma)$ is the Thomson scattering amplitude of electrons scattering a wave from direction $\hat{p}_{\beta\sigma}$ to $\hat{p}_{\alpha\beta}$. Finally,

$$f_{il}(\alpha\beta,\beta 0) = f_0\, \hat{e}_{\alpha\beta}(i)\cdot\hat{e}(1)$$

is the scattering of the incident wave by the electron at $\underset{\sim}{z}_\beta$. If we sequentially substitute the right-hand side into the left-hand side of Eq. (4), we obtain the series

$$\underset{\sim}{E}(\alpha) = \underset{\sim}{E}_I(\alpha) + \sum_{\beta(\neq\alpha)=1}^{N} \Bigg\{ \sum_{j=1}^{2} \hat{e}_{\alpha\beta}(j)\, G_{\alpha\beta}{}^0\, f_{jl}(\alpha\beta,\beta 0)\, E_I(\beta)$$

$$+ \sum_{j=1}^{2} \hat{e}_{\alpha\beta}(j) \sum_{\sigma(\neq\beta)=1}^{N} \sum_{i=1}^{2} G_{\alpha\beta}{}^0\, f_{ji}(\alpha\beta,\beta\sigma)\, G_{\beta\sigma}{}^0\, f_{il}(\beta\sigma,\sigma 0)\, E_I(\sigma)$$

$$+ \cdots \Bigg\} \,.$$

The first term represents the incident wave, the second term the once-scattered wave, the third term the twice-scattered wave, etc.

What we actually want to calculate is the average power of the field. The average of any quantity $A(1,2,\cdots N)$ of N particles is defined by

$$\langle A \rangle = \int A(1,2,\cdots N)\, P_N(1,2,\cdots N)\, d^3Z_1\, d^3Z_2 \cdots d^3Z_N,$$

where P_N is the N-particle distribution function. Conventionally,

$$P_2(1,2) = P_1(1)\, P_1(2)[1 + g(12)] , \qquad (5)$$

where $g(12)$ is the two-particle correlation function. And $P_3, P_4, \cdots P_N$ all can be written in similar form. In our problem, it is convenient to separate the averaging process according to the statistical correlation between the electrons into a coherent part and an incoherent part. The coherent wave $\underset{\sim}{E}_c = \langle \underset{\sim}{E} \rangle$ is

$$\underset{\sim}{E}_c(\alpha) = \underset{\sim}{E}_I(\alpha) + f_0 \sum_{\beta} \int P_1(\beta)\, G_{\alpha\beta}^{0}\, \underset{\sim}{E}_I(\beta)\, d^3Z_\beta$$

$$+ \sum_{\beta_1\beta_2} f_0^2 \int P_1(\beta_1) P_1(\beta_2)\, G^0_{\alpha\beta_1}\, G^0_{\beta_1\beta_2}\, \underset{\sim}{E}_I(\beta_2)\, d^3Z_{\beta_1}\, d^3Z_{\beta_2} + \cdots$$

$$= \underset{\sim}{E}_I(\alpha) + \int d^3 Z_\beta\, \rho(\beta)\, f_0\, G_{\alpha\beta}^{0}\, \underset{\sim}{E}_c(\beta) , \qquad (6)$$

where we have denoted the average electron density by $\rho(\underset{\sim}{Z}) = N\, P_1(\underset{\sim}{Z})$, which is justified when $N \gg 1$.

In order to simplify the problem, we assume (1) $|1 - n| \ll 1$, where n is the refractive index; the plasma is underdense, (2) the size of the plasma r_s is much greater than the wavelength of the incident field, i.e., $k_{in} r_s \gg 1$, so that the coherent scattering of waves only occurs in the forward direction, (3) $k_{in} \gg |\underset{\sim}{\nabla} \ell n\, n|$, the eikonal approximation of wave propagation may be used. The coherent wave then satisfies the following equation

$$[\underset{\sim}{\nabla}_\alpha^2 + k_{in}^2\, n^2(\alpha)]\, \underset{\sim}{E}_c(\alpha) = 0 ;$$

$$n^2(\underset{\sim}{Z}) = 1 + \frac{4\pi}{k^2} \left[f_0\, \rho(\underset{\sim}{Z}) + \rho^2(\underset{\sim}{Z}) \int d^3R\, g(\underset{\sim}{Z},R) \right.$$

$$\left. \exp[n_1(\underset{\sim}{Z})(\underset{\sim}{k}_{in} - k_{in}\hat{p})\cdot R]/R \sum_{j=1}^{2} [f_{j1}(\hat{k}_{in},\hat{p})]^2 \right] \qquad (7)$$

where

$$n_1^2(\underset{\sim}{Z}) = 1 + \frac{4\pi}{k^2} f_0\, \rho(\underset{\sim}{Z}) = 1 - \frac{\omega_p^2}{\omega^2}$$

is the first-order approximation of $n^2(\underset{\sim}{Z})$, $\hat{p}$ is a dummy vector inside the correlation cell, and $n^2(\underset{\sim}{Z})$ is independent of $\hat{p}$. The solution of the coherent wave is

$$\underset{\sim}{E}_c(\alpha) \approx \exp\left[i \int_{\hat{k}_{in}}^{\underset{\sim}{Z}_\alpha} \underset{\sim}{X}\, k_{in}\, n\, ds \right] \cdot \underset{\sim}{E}_I(\underset{\sim}{X})$$

where $\int_{\hat{k}_{in}}$ means the integral along the path parallel to the incident direction $\hat{k}_{in}$.

After we have the coherent part solved, let us go back to Eq. (1). The total field can now be written as the following

$$\underset{\sim}{E}(\alpha) = \underset{\sim}{E}_c(\alpha) + \sum_{\beta(\neq\alpha)=1}^{N} \sum_{j=1}^{2} \hat{e}_{\alpha\beta}(j)\, E'_{\alpha\beta}(j) \ .$$

The average power of the field is

$$P(\alpha,\hat{e}) = \frac{c}{8\pi} \langle |\hat{e}\cdot\underset{\sim}{E}(\alpha)|^2 \rangle$$

or

$$P(\alpha,\hat{e}) = P_c(\alpha,\hat{e}) + \sum_{\beta_1,\beta_2} \sum_{i,j=1}^{2} \left\langle \hat{e}\cdot\hat{e}_{\alpha\beta_1}(i)\ \hat{e}\cdot\hat{e}_{\alpha\beta_2}(j) \times \frac{E'^{*}_{\alpha\beta_1}(i)\, E'_{\alpha\beta_2}(j)}{8\pi} \right\rangle \ , \qquad (8)$$

where

$$P_c(\alpha,\hat{e}) = \frac{c}{8\pi} |\hat{e}\cdot\underset{\sim}{E}_c(\alpha)|^2 \ .$$

In other words,

$$P_c(\alpha,\hat{e}) = \frac{c}{8\pi}|E_0|^2 \exp\left(- \int_{\hat{k}_{in}}^{Z_\alpha} \underset{\sim}{X}\, 2(\mathrm{Im}\ n)\, k_{in} ds \right) (\hat{e}\cdot\hat{e}(1))^2$$

$$= \frac{c}{8\pi}|E_0|^2 \exp\left(- \int_{\hat{k}}^{Z_\alpha} \underset{\sim}{X}\, \frac{ds}{\ell} \right) (\hat{e}\cdot\hat{e}(1))^2$$

where

$$\frac{1}{\ell(Z)} = 2\, k_{in}\, \mathrm{Im}(n) = \rho^2(Z) \int d\Omega_{\hat{p}} \int d^3R\ g(Z,R)$$

$$\times\ e^{i n_1(Z)(k_{in}\hat{p}-k_{in})\cdot R} \sum_{j=1}^{2} (f_{j1}(\hat{k}_{in}\cdot\hat{p}))^2 \ . \qquad (9)$$

We usually call ℓ the scattering mean free path. The second term in Eq. (8) corresponds to the incoherent part. It was manipulated under the assumption of $R_c \ll \ell$, where R_c is the correlation length between the electrons, giving us the following approximation

$$\int_{Z_\beta}^{Z_{\alpha'}} n(\underset{\sim}{x})\, ds \sim \int_{Z_\beta}^{Z_\alpha} n(\underset{\sim}{x})\, ds + n(\underset{\sim}{Z}_\alpha)\, \hat{R}_{\alpha\beta}\cdot(\underset{\sim}{Z}_{\alpha'} - \underset{\sim}{Z}_\alpha) \qquad (10)$$

when $|\underset{\sim}{Z}_{\alpha'} - \underset{\sim}{Z}_\alpha| \approx 0\ (R_c)$ and $|\underset{\sim}{Z}_\alpha - \underset{\sim}{Z}_\beta| = R_{\alpha\beta} \approx 0\ (\ell)$. Equation (10) means we may consider that the electric field of a wave remains the same within each group of electrons of size R_c. And the successive scattering occurs at the wave zone of each of these groups. A more explicit expression for $R_c \ll \ell$ may be obtained from Eq. (9):

$$\frac{R_c}{\ell} = 0\left[\frac{\omega_p^4}{\omega^4} \frac{\langle (\rho - \bar{\rho})^2 \rangle}{\bar{\rho}^2} \right] \ll 1 \ . \qquad (11)$$

We found the incoherent part of the power to be

$$P_{incoh} = \sum_{i,j=1}^{2} d^3Z_\beta\ \hat{e}\cdot\hat{e}_{\alpha\beta}(i)\ \hat{e}\cdot\hat{e}_{\alpha\beta}(j)\ P_{ij}(\alpha,\beta) \qquad (12)$$

with

$$P_{ij}(\alpha,\beta) = \int d^3Z_{\beta_1}\, d^3Z_{\beta_2}\, \delta\left(\frac{1}{2}(Z_{\beta_1} + Z_{\beta_2}) - Z_\beta\right) \rho(\beta_1)\, \rho(\beta_2)$$

$$\times\, g(\beta_1\beta_2) \left\langle \frac{E'^{*}_{\alpha\beta_1}(i)\, E'_{\alpha\beta_2}(j)}{8\pi} \right\rangle_{\alpha\beta_1\beta_2} , \qquad (13)$$

where $\langle\cdots\rangle_{\alpha\beta_1\beta_2}$ is the average over all the particles except α, β_1, and β_2.

We introduce the Stokes parameters for a wave $\underset{\sim}{I}$ propagated in direction $\hat{p}$ (we change $\alpha\beta$ etc. to $\hat{p}$, $\hat{p}'$):

$$\underset{\sim}{I}(\hat{p}) = \begin{pmatrix} E^*_p(1)\, E_p(1) \\ E^*_p(2)\, E_p(2) \\ E^*_p(1)\, E_p(2) \\ E^*_p(2)\, E_p(1) \end{pmatrix} = \frac{1}{c} \begin{pmatrix} P_{11} \\ P_{22} \\ P_{12} \\ P_{21} \end{pmatrix} = \begin{pmatrix} I_{11} \\ I_{22} \\ I_{12} \\ I_{22} \end{pmatrix}$$

we obtain from Eqs. (8), (12), and (13)

$$\underset{\sim}{I}(\underset{\sim}{X},\hat{p}) = \underset{\sim}{I}_0\, e^{-\int_{\hat{k}_{in}} \frac{ds}{\ell}}\, \delta_{\hat{k}_{in},\hat{p}} + \int_{-\hat{p}} ds(\underset{\sim}{Z}) \exp\left(-\left|\int_{\hat{p}\,\underset{\sim}{Z}}^{\underset{\sim}{X}} \frac{ds}{\ell}\right|\right)$$

$$\times \int d\Omega_{\hat{p}'}\; \underset{\sim}{\underset{\sim}{M}}(\hat{p},\hat{p}',\underset{\sim}{Z})\, \underset{\sim}{I}(\underset{\sim}{Z},\hat{p}') , \qquad (14)$$

where $\underset{\sim}{I}_0 = \left((I_0)_{ij}\right) = \left(E^*_0(i)\, E_0(j)\right)$, and $\underset{\sim}{\underset{\sim}{M}}$ is a 4×4 matrix defined by

$$(st|\underset{\sim}{\underset{\sim}{M}}(\hat{p},\hat{p}',\underset{\sim}{x})|ij) = \sigma_g(\hat{p}\cdot\hat{p}',\underset{\sim}{x})\left(\hat{e}_{\hat{p}}(s)\cdot\hat{e}_{\hat{p}'}(i)\right)\left(\hat{e}_{p}(t)\cdot\hat{e}_{\hat{p}'}(j)\right)$$

with

$$\sigma_g(\hat{p}\cdot\hat{p}\cdot\underset{\sim}{x}) = f_0^{\,2}\, \rho^2(\underset{\sim}{x}) \int d^3R\; g_2(\underset{\sim}{Z},R)\; e^{i n_1(\underset{\sim}{Z}) k(\hat{p}-\hat{p}')\cdot R} .$$

The equivalent differential form of Eq. (14) is

$$\frac{\partial I(\hat{p},\underset{\sim}{X})}{\partial s} + \frac{I(\hat{p},\underset{\sim}{X})}{\ell(\underset{\sim}{X})} = \int \underset{\sim}{\underset{\sim}{M}}(\hat{p}\cdot\hat{p}',\underset{\sim}{X})\, \underset{\sim}{I}(\hat{p}',\underset{\sim}{X})\, d\Omega_{\hat{p}'} . \qquad (15)$$

This is the familiar transport equation.

We want to point out here that Watson's derivation of the transport equation (stated above) gives us definite information about the dependence of the scattering mean free path ℓ on the properties of the scattering medium through σ_g, in contrast to the "guessing" required in the ordinary phenomenological derivation.

3. CORRELATION FUNCTION FOR TURBULENT MEDIUM

The two-particle correlation, which is the most relevant part in the transport equation, depends totally on the characteristics of the medium. It thus serves two purposes. One is to predict the power or polarization of the scattered wave for a medium whose properties are known. The other one is to find out the characteristic properties of a medium by looking at the experimental data of the waves scattered from this medium.

An underdense turbulent plasma is one for which the plasma frequency of the medium is much smaller than the incident wave frequency. If the collisional frequencies ν_{in} between the ions and the neutrals are high enough so that $|(dv_n)/(dt)| \ll \nu_{in} v_n$,[10] where v_n is the medium velocity of the neutrals, the ions will follow the neutrals. But electrons are usually following the ions; so the correlation between the electrons in the medium is just the same as that of the neutrals, which should obey the ordinary turbulent fluid theory. Let us start from the diffusion equation in fluid dynamics

$$\frac{\partial \rho}{\partial t} + \nabla\cdot(\underset{\sim}{u}\rho - \mathcal{D}\nabla\rho) = 0 , \qquad (16)$$

ρ is the number density of particles, $\underset{\sim}{u}$ is the velocity of the medium, and $\mathcal{D}$ is the ambipolar diffusion coefficient for electrons and ions that are moving together in the medium. The third term $(\mathcal{D}\nabla\rho)$ in Eq. (16) represents the flow of the electrons caused by diffusion through the neutrals, while the second term $(u\rho)$ is the flow caused by medium motion. If we set $\rho = \rho(x)$, $\rho' = \rho(x')$, then from Eq. (16) we may obtain

$$\frac{\partial}{\partial t}\langle\rho\rho'\rangle + \nabla_R\cdot\langle u\rho\rho'\rangle - \nabla_R\cdot\langle u'\rho'\rho\rangle = \mathcal{D}\nabla_R^2\langle\rho\rho'\rangle . \qquad (17)$$

We have simplified the problem by assuming a homogeneous medium such that $\langle\rho\rho'\rangle$ and $\langle u\rho\rho'\rangle$ are functions of $R = (x - x')$ only, and $\mathcal{D}$ is a constant. Then the Kolmogoroff's[11] dimensional analysis argument can be followed exactly, except that the velocity variable is replaced by a conservative, passive, additive quantity--density.[12] In the following, we will derive the results claimed by Tatarski[13] in 1961.

If we Fourier transform Eq. (17) into k-space, letting

$$S(k) = \frac{1}{(2\pi)^{3/2}}\int \langle\rho\rho'\rangle(R)\, e^{ik\cdot R}\, d^3R$$

$$\Gamma(k) = \frac{1}{(2\pi)^{3/2}}\int \left\{\nabla_R\cdot[\langle u\rho\rho'\rangle - \langle u'\rho'\rho\rangle](R)\right\} e^{ik\cdot R}\, d^3R ,$$

we get

$$\frac{\partial}{\partial t} S(k) + \Gamma(k) = -2\mathcal{D}k^2 S(k) . \qquad (18)$$

It is easily proved that $\int \Gamma(k)\, d^3k = 0$.[14] That is to say, $\Gamma(k)$--the coupling between ρ and u--transfers the $\langle\rho\rho'\rangle$-stuff between different k-spaces, but the total $\langle\rho\rho'\rangle$-stuff is conserved. So there is a region in k-space, when $k_0 \ll k \ll k_d$, where $S(k)$ should be isotropic and depends only on two parameters. One is $\chi = \mathcal{D}\nabla^2\langle\rho\rho'\rangle$, which corresponds to the dissipation of $\langle\rho\rho'\rangle$-stuff by diffusion. The other one is the rate of dissipation of the turbulent energy ϵ, which is directly related to the velocity of the turbulent medium u,

which in turn affects the transfer of the $\langle \rho\rho' \rangle$-stuff. The upper and lower limits for the isotropic region are usually defined by

$$k_0 \sim \frac{1}{r_s}$$

$$k_d \sim \frac{1}{r_\alpha} ,$$

where r_s is the size of the largest eddy in the medium, generally the same order of magnitude as the size of the plasma, and

$$r_d \sim \left(\frac{\mathcal{D}^3}{\epsilon}\right)^{\frac{1}{4}} .$$

Dimension-wise, letting L be length and t be time, we have

$$[S(k)] = \left[\frac{t^2}{L^6} \cdot L^3\right] = \left[\frac{t^2}{L^3}\right] ,$$

$$[\chi] = [\mathcal{D}][\nabla^2\langle \rho\rho' \rangle] = \left[\frac{t}{L^6}\right] .$$

Thus,

$$[S(k)] = [\chi][L^3 t]\, f(kL) = [\chi][L^3 t][kL]^\alpha$$

$$= [\chi]\left[\frac{\mathcal{D}^3}{\epsilon}\right]^{\frac{4+\alpha}{4}} [\mathcal{D}\epsilon]^{-\frac{1}{4}} k^\alpha .$$

Since $S(k)$ only depends on χ and ϵ, there should be no explicit dependence on $\mathcal{D}$; we obtain

$$\alpha = -\frac{11}{3} .$$

Thus

$$S(k) \propto k^{-\frac{11}{3}} \quad \text{when} \quad k_0 \ll k \ll k_d . \tag{19}$$

Looking at the last term of Eq. (18), we recall that the dissipation effects due to diffusion heavily dominate in the large-k region because of the k^2 dependence. Batchelor[12] found that

$$S(k) \propto \exp(-k^2/\text{constant}) \quad \text{when} \quad k \gg k_d , \tag{20}$$

i.e., the eddies at large k diminish very fast.

4. SOLUTION OF VECTOR TRANSPORT EQUATION

4.1. Discrete Coordinate Method

The general way to solve the scalar transport equation is either by spherical harmonic expansion or by the Gaussian discrete-coordinate method. It was proved[15] that the two methods are equivalent for plane geometry. In other geometries, such as cylindrical or spherical geometry, there will be a differential term $\frac{\partial I}{\partial \mu}$ present in the transport equation, where μ is the angle variable $\cos\theta$. Since numerical differentiation is rather inaccurate generally, the discrete coordinate method is unlikely to be superior to the spherical-harmonic method.

For the vector transport equation, the case of constant scattering function has been tried.[16] Our problem involves not only a matrix concerning the polarization effect, but also a scattering function σ_g. Both of them depend on the direction angles of the incoming direction $\hat{p}$ and the scattering direction $\hat{p}'$. It is too cumbersome to write every matrix element multiplied by σ_g into an expansion of spherical harmonics. Not only so, the multiplication of the matrix by the Stokes column vector will complicate the calculation even more. It seemed to be reasonable to go to the much simpler discrete-coordinates method, which would give the same accuracy in the nth-order approximation as would the nth-order spherical-harmonic expansion[15] for plane geometry.

The scattering matrix $\underset{\sim}{M}'$ in the transport equation

$$\frac{\partial}{\partial s}\underset{\sim}{I}'(\hat{p}) + \frac{1}{\ell}\underset{\sim}{I}'(\hat{p}) = \int \underset{\sim}{M}'(\hat{p},\hat{p}')\cdot\underset{\sim}{I}'(\hat{p}')\, d\Omega_{\hat{p}'}$$

is defined by

$$\langle st|\underset{\sim}{M}'(\hat{p},\hat{p}')|ij\rangle = \sigma_g(\hat{p},\hat{p}')[\hat{e}_{\hat{p}}(s)\cdot\hat{e}_{\hat{p}'}(i)][\hat{e}_{\hat{p}}(t)\cdot\hat{e}_{\hat{p}'}(j)] .$$

In our problem, for the sake of convenience, we changed the basis

$$\underset{\sim}{I}' = \begin{bmatrix} E_1^* E_1 \\ E_2^* E_2 \\ E_1^* E_2 \\ E_2^* E_1 \end{bmatrix} = \begin{bmatrix} |E_1|^2 \\ |E_2|^2 \\ |E_1||E_2|\exp(i\delta) \\ |E_2||E_1|\exp(-i\delta) \end{bmatrix}$$

to

$$\underset{\sim}{I} = \begin{bmatrix} |E_1|^2 \\ |E_2|^2 \\ 2E_1E_2\cos\delta \\ 2E_1E_2\sin\delta \end{bmatrix}, \qquad (21)$$

where δ is the phase difference between E_1 and E_2,

$$\underset{\sim}{I} = \underset{\sim}{A}\cdot\underset{\sim}{I}'$$

where

$$\underset{\sim}{A} = \begin{bmatrix} 1 & 0 & 0 & 0 \\ 0 & 1 & 0 & 0 \\ 0 & 0 & \frac{1}{2} & \frac{i}{2} \\ 0 & 0 & \frac{1}{2} & -\frac{i}{2} \end{bmatrix}$$

The corresponding change in the matrix $\underset{\sim}{M}$ is

$$\underset{\sim}{M} = \underset{\sim}{A}^{-1} \cdot \underset{\sim}{M}' \cdot \underset{\sim}{A} ;$$

the elements in $\underset{\sim}{M}$ are listed in Table I. The angles (θ,ϕ), (θ',ϕ') are the direction angles for $\hat{p}$ and $\hat{p}'$, respectively.

For a plane homogeneous plasma, we have $\sigma_g(\hat{p}\cdot\hat{p}')$ depending only on $(\hat{p} - \hat{p}')$. We transformed it into a Fourier series

$$\sigma_g(\hat{p} - \hat{p}') = \sum_{\lambda} \sigma_{c\lambda} \cos\big(\lambda(\phi' - \phi)\big) + \sigma_{s\lambda} \sin\big(\lambda(\phi' - \phi)\big).$$

We also separated the matrix elements in $\underset{\sim}{M}$ into five 4×4 submatrices according to the sine and cosine function of angle $(\phi' - \phi)$; thus

$$\underset{\sim}{M} = \left[\sum_{\lambda} \sigma_{c\lambda} \cos\big(\lambda(\phi' - \phi)\big) + \sigma_{s\lambda} \sin\big(\lambda(\phi' - \phi)\big)\right] \times \Big[\underset{\sim}{M}_0(\theta,\theta') + \underset{\sim}{M}_{c1}(\theta,\theta') \cos(\phi' - \phi) + \underset{\sim}{M}_{s1}(\theta,\theta') \sin(\phi' - \phi) + \underset{\sim}{M}_{c2}(\theta,\theta') \cos\big(2(\phi' - \phi)\big) + \underset{\sim}{M}_{s2}(\theta,\theta') \sin\big(2(\phi' - \phi)\big)\Big] \tag{22}$$

where $\underset{\sim}{M}_0$ is that part of the matrix that has no dependence on $(\phi' - \phi)$. Let the wave vector $\underset{\sim}{I}(\hat{p})$ be written as a summation of the coherent wave and an incoherent wave

$$\underset{\sim}{I}(\hat{p}) = \underset{\sim}{I}_c + \underset{\sim}{\Phi}(\hat{p}) = \underset{\sim}{I}_0 \exp\left(-\int_{\hat{k}_{in}} \frac{ds}{\ell}\right) \delta_{\hat{k}_{in},\hat{p}} + \underset{\sim}{\Phi}(\hat{p}) . \tag{23}$$

Substituting into the transport equation, we get

$$\frac{\partial}{\partial s} \underset{\sim}{\Phi}(\hat{p}) + \frac{1}{\ell} \underset{\sim}{\Phi}(\hat{p}) = \underset{\sim}{M}(\hat{p},\hat{k}_{in}) \cdot \underset{\sim}{I}_0 \exp\left(-\int_{\hat{k}_{in}} \frac{ds}{\ell}\right) + \int \underset{\sim}{M}(\hat{p},\hat{p}') \, \underset{\sim}{\Phi}(\hat{p}') \, d\Omega_{\hat{p}'} . \tag{24}$$

We expand the column vector $\underset{\sim}{\Phi}(\hat{p})$ into a Fourier series

$$\underset{\sim}{\Phi}(\hat{p}) = \sum_{m} \underset{\sim}{\Phi}_{cm}(\theta) \cos(m\phi) + \underset{\sim}{\Phi}_{sm}(\theta) \sin(m\phi) . \tag{25}$$

Replace every term in Eq. (24) by its Fourier series and integrate over ϕ'. We obtain for each integer m the following equation

$$\left(\ell \frac{\partial}{\partial s} + 1\right) \begin{bmatrix} \underset{\sim}{\Phi}_{cm}(\theta) \\ \underset{\sim}{\Phi}_{sm}(\theta) \end{bmatrix} = \frac{\ell}{2} e^{-\int_{\hat{k}_{in}} \frac{ds}{\ell}} \underset{\sim}{\eta}(\theta,\theta_k) \cdot \begin{bmatrix} \underset{\sim}{I}_0 \sin(m\phi_k) \\ \underset{\sim}{I}_0 \cos(m\phi_k) \end{bmatrix} + \frac{\ell\pi}{2} \int \underset{\sim}{\eta}(\theta,\theta') \cdot \begin{bmatrix} \underset{\sim}{\Phi}_{cm}(\theta') \\ \underset{\sim}{\Phi}_{sm}(\theta') \end{bmatrix} d(\cos\theta') , \tag{26}$$

where (θ_k,ϕ_k) are the direction angles of the incident direction $\hat{k}_{in}$ and

$$\underset{\sim}{\eta}(\theta,\theta') = \begin{bmatrix} \underset{\sim}{M}_{ccm}(\theta,\theta') & \underset{\sim}{M}_{csm}(\theta,\theta') \\ \underset{\sim}{M}_{scm}(\theta,\theta') & \underset{\sim}{M}_{ssm}(\theta,\theta') \end{bmatrix}$$

is a 8×8 matrix with

$$\underset{\sim}{M}_{scm}(\theta,\theta') = \underset{\sim}{M}_{csm}(\theta,\theta')$$

$$= 2\,\sigma_{sm}\,\underset{\sim}{M}_{0}(\theta,\theta')$$

$$+ \sum_{J=1}^{2}\left[\left(\sigma_{s(m-J)} + \sigma_{s(m+J)}\right)\underset{\sim}{M}_{cJ}(\theta,\theta')\right.$$

$$\left. + \left(\sigma_{c(m-J)} - \sigma_{c(m+J)}\right)\underset{\sim}{M}_{sJ}(\theta,\theta')\right]$$

and

$$\underset{\sim}{M}_{ssm}(\theta,\theta') = \underset{\sim}{M}_{ccm}(\theta,\theta')$$

$$= 2\,\sigma_{cm}\,\underset{\sim}{M}_{0}(\theta,\theta')$$

$$+ \sum_{J=1}^{2}\left[\left(\sigma_{c(m-J)} + \sigma_{c(m+J)}\right)\underset{\sim}{M}_{cJ}(\theta,\theta')\right.$$

$$\left. + \left(\sigma_{s(m+J)} - \sigma_{s(m-J)}\right)\underset{\sim}{M}_{sJ}(\theta,\theta')\right] .$$

Denoting

$$\begin{bmatrix} \phi_{cm}(\theta) \\ \phi_{sm}(\theta) \end{bmatrix} \quad \text{by} \quad \underset{\sim}{\phi}_{m}(\theta),$$

and

$$\underset{\sim}{M}(\theta,\theta_k)\begin{bmatrix} I_{0} \sin m\phi_k \\ I_{0} \cos m\phi_k \end{bmatrix} \quad \text{by} \quad \underset{\sim}{H}_{m}(\theta),$$

we obtain from Eq. (26) the modified transport equation

$$\ell\,\frac{\partial}{\partial s}\,\underset{\sim}{\phi}_{m}(\theta) + \underset{\sim}{\phi}_{m}(\theta) = \frac{\ell}{2}\exp\left(-\int_{\hat{k}_{in}}\frac{ds}{\ell}\right)\underset{\sim}{H}_{m}(\theta)$$

$$+ \frac{\ell_{\pi}}{2}\int \underset{\sim}{\mathcal{M}}(\theta,\theta')\,\underset{\sim}{\phi}_{m}(\theta')\,d(\cos\theta') . \qquad (27)$$

So far, we have separated the equation from the dependence on ϕ and are left with θ only. Now we are in the position to apply the discrete-coordinates method in which the integral may be changed to a summation

$$\int \underset{\sim}{\mathcal{M}}(\theta,\theta')\cdot\underset{\sim}{\phi}_{m}(\theta')\,d(\cos\theta') \approx \sum_{j=1}^{N} A_j\,\underset{\sim}{\mathcal{M}}(\mu,\mu_j)\cdot\underset{\sim}{\phi}_{m}(\mu_j)$$

where $\mu = \cos\theta$, and μ_j's and A_j's are the divisions and weights of the quadrature summation formula.[17] Among the various methods, the values of the Gaussian formula are given in Table II. Equation (27) is transformed into a system of linear differential equations

$$\ell\,\frac{\partial}{\partial s}\,\underset{\sim}{\phi}_{m}(\mu_i) + \underset{\sim}{\phi}_{m}(\mu_i) = \frac{\ell}{2}\exp\left(-\int_{\hat{k}_{in}}\frac{ds}{\ell}\right)\underset{\sim}{H}_{m}(\mu_i)$$

$$+ \frac{\ell_{\pi}}{2}\sum_{j=1}^{N} A_j\,\underset{\sim}{\mathcal{M}}(\mu_i,\mu_j)\cdot\underset{\sim}{\phi}_{m}(\mu_j) , \qquad i=1\cdots N . \qquad (28)$$

To solve the equations, let the inhomogeneous solution be

$$\underset{\sim}{h}_{m}(\mu_i)\exp\left(-\int_{\hat{k}_{in}}\frac{ds}{\ell}\right) ,$$

and the homogeneous solution be $\underset{\sim}{g}_{m}(\mu_i)\,e^{kr}$, where

$$r = \int_{-\infty}^{z} \frac{dz}{\ell(z)} \tag{29}$$

under the assumption that the particle density depends only on the z coordinate and that $\ell = \ell(z)$. The z-axis is taken to be perpendicular to the slab. We then obtain

$$\underset{\sim}{\Phi}_m(\mu_i) = \underset{\sim}{h}_m(\mu_i)\, e^{-r/\mu_k} + \sum_{\lambda=1}^{8N} C_\lambda\, \underset{\sim}{g}_{m\lambda}(\mu_i)\, e^{k_\lambda r} ,$$

where k_λ's are the eigenvalues of the matrix

$$\frac{\ell\pi}{2} \sum_{j=1}^{N} A_j\, \underset{\sim}{\mathcal{M}}_l(\mu_i,\mu_j) - (k + \tfrac{1}{\ell})\, \delta_{ij}\, \underset{\sim}{1} = 0 . \tag{30}$$

The $\underset{\sim}{1}$ is the identity matrix; the C_λ's are constants which need to be determined by boundary conditions.

After we have solved the differential equations for each integer m, the total intensity of the wave scattered in direction (μ_i,ϕ_i) is then

$$\underset{\sim}{I}(\mu_i,\phi_i) = \sum_m [\underset{\sim}{\Phi}_{cm}(\mu_i) \cos(m\phi_i) + \underset{\sim}{\Phi}_{sm}(\mu_i) \sin(m\phi_i)]$$

$$+ \underset{\sim}{I}_0 \exp\left(-\int_{\hat{k}_{in}} \frac{ds}{\ell}\right) \delta_{\mu_i,\mu_k}\, \delta_{\phi_i,\phi_k} .$$

We may substitute the intensity $\underset{\sim}{I}$ calculated above from the differential transport Eq. (15) back into the integral transport

Eq. (14). If $\underset{\sim}{I}$ is the exact solution of (15), the two results should be identical. This is one way to check the accuracy of our approximation.

4.2. Boundary Conditions

In the above calculation, we have separated the wave into a coherent and an incoherent part [see Eq. (23)]. At the surface exposed to the incident wave, it is equivalent to separate the wave into a part that comes from outside directly and a part which has undergone at least one scattering in the medium. As far as the scattering wave is concerned, we may consider this surface, as well as any other surfaces bounding the plasma, as a free surface. So both Mark's[18] and Marshak's boundary conditions can be applied.

For a free surface at $x = 0$ such that the medium occupies the space $x < 0$, the boundary conditions are

$$\Phi(0,\mu) = 0 \qquad \text{for } \mu \geq 0.$$

This constitutes an infinite number of conditions, which cannot all be exactly satisfied in an approximation of finite order. In the Nth-order approximation, if we take N odd, we can only satisfy $\frac{1}{2}(N + 1)$ conditions. (The rest have to go with the angles that $\mu < 0$.) Mark's boundary conditions specify choosing a set of definite μ_j's such that

$$\Phi(0,\mu_j) = 0 \qquad [j = 1,2,\cdots\tfrac{1}{2}(N + 1)].$$

One of his choices is to take μ_j's from the roots of the Legendre polynomials P_{N+1} such that

$$P_{N+1}(\mu_j) = 0.$$

Marshak's boundary conditions specify choosing the set of orthogonal Legendre polynomials $P_{2j-1}(\mu)$ so that we have

$$\int_0^1 \Phi(0,\mu)\, P_{2j-1}(\mu)\, d\mu = 0 \quad [j = 1,2,\cdots\tfrac{1}{2}(N+1)] .$$

This includes the condition of conservation of the numbers of photons

$$\int_0^1 \Phi(0,\mu)\, \mu d\mu = 0 ;$$

the total flux of photons entering the system is zero.

Although Marshak's boundary conditions are better in the lower-order approximation, in the discrete-coordinate method the integral involves in his condition has to be replaced by a summation. And the confusion in making the $\frac{1}{2}(N+1)$ choices of angles μ_j in Mark's condition no longer exists in the discrete-coordinate approximation. Thus we set the boundary conditions for plane geometry by following Mark's rules. That is, at the incident surface $r = 0$

$$\Phi_m(\mu_i) = 0 , \qquad 0 \le \mu_i \le 1;$$

at the other boundary surface of the slab $r = D$

$$\Phi_m(\mu_i) = 0 \quad \text{and} \quad 0 \ge \mu_i \ge -1 .$$

This will give us $8N$ boundary conditions which will determine the $8N$ constants, c_λ's.

5. BACKSCATTERING FROM SLAB GEOMETRY

5.1. Modification of Transport Equation

When the transport equation

$$\frac{\partial}{\partial s}\, \underset{\sim}{I}(\hat{p}) + \frac{1}{\ell}\, \underset{\sim}{I}(\hat{p}) = \int \underset{\sim}{M}(\hat{p},\hat{p}')\cdot \underset{\sim}{I}(\hat{p}')\, d\hat{p}'$$

is solved, we in principle should get the intensity in all directions $\hat{p}$. But for backscattering there are some difficulties. From the definitions in Eqs. (2) and (4), we have

$$f_{ij}(-\hat{p},-\hat{q}) = f_0\, \hat{e}_{-\hat{p}}(i)\cdot\hat{e}_{-\hat{q}}(j) = f_{ji}(\hat{q}\cdot\hat{p})(-1)^{i+j} . \qquad (31)$$

That is to say, for a given path in multiple scattering, if we reverse the direction along the path, the scattering amplitude of each scattering will have the interesting change given by Eq. (31). The total interference effect of the two directions along this path was shown in Ref. 5. If the wave solution from the transport equation $\underset{\sim}{I}_1(-\hat{k}_{in})$ is

$$\underset{\sim}{I}_1(-\hat{k}_{in}) = \underset{\sim}{T}\cdot\underset{\sim}{I}_0(\hat{k}_{in}) ,$$

and we let the true backscattered power $\underset{\sim}{I}(-\hat{k}_{in})$ be

$$\underset{\sim}{I}(-\hat{k}_{in}) = \underset{\sim}{\mathcal{J}}\cdot\underset{\sim}{I}_0(\hat{k}_{in})$$

and define a matrix $\underset{\sim}{B}$ as

$$\underset{\sim}{I}_2(-\hat{k}_{in}) = + \int_{-\hat{k}_{in}} \underset{\sim}{M}(-\hat{k}_{in},\hat{k}_{in})\cdot\underset{\sim}{I}_0(\hat{k}_{in}) \exp\left(-2\left|\int_{\hat{k}_{in}} \frac{ds}{\ell}\right|\right) ds$$

$$= \underset{\sim}{B}\cdot\underset{\sim}{I}_0(\hat{k}_{in}) ,$$

then for

$$\underset{\sim}{T} = \underset{\sim}{B} + \underset{\sim}{\Delta T}$$

we have

$$(ij|\mathcal{T}|st) = (ij|T|st) + \frac{1}{2}\Big\{(-1)^{i+s}\,(sj|\Delta T|it) + (-1)^{j+t}\,(it|\Delta T|sj)\Big\}\,, \qquad (32)$$

which after being transformed into our representation [Eq. (21)] are listed in Table III.

The medium we are considering is an underdense turbulent plasma. Because collision frequencies between electrons and neutrals are usually much higher than those between electrons and ions, we may neglect the effect of ion-electron collision, and consider only the absorption due to electron-neutral collisions, plus the scattering loss. When the average collision frequency ν_c is small compared with the frequency ω of the incident wave, we may approximate ω by $\omega + i\nu_c$ in our scattering theory. As a result, there are a few changes in the expressions of our defined parameters, the most obvious ones being the Thomson scattering amplitude

$$f_0 \to \frac{-e^2}{mc^2\left(1 + \frac{\nu_c^2}{\omega^2}\right)}$$

and the real part of the square of the refractive index

$$n_1^2 \to 1 - \frac{\omega_p^2}{(\omega^2 + \nu_c^2)}\,.$$

The imaginary part of the refractive index, which in turn defines the scattering mean free path ℓ, now has an extra term added to the original one related to the spectral function [see Eq. (9)]. Let us denote the scattering part from now on by ℓ_t; the total scattering mean free path ℓ then satisfies the following relation

$$\frac{1}{\ell} = 2(I_m\, n)\, k_{in} = \frac{1}{\ell_t} + \frac{1}{\ell_c}\,,$$

where

$$\frac{1}{\ell_t} = \rho^2 \int d\Omega_{\hat{p}'} \cdot \int d^3R\; g(R)\; e^{in_1 k_{in}(\hat{p}-\hat{p}')\cdot R} \sum_{j=1}^{2} f_{ji}(\hat{p}\cdot\hat{p}')$$

$$= \rho^2 f_0^2 \int d\Omega_{\hat{p}'}\; \sigma_g(\hat{p},\hat{p}')\left[\frac{1}{2}\left(1 + (\hat{p}\cdot\hat{p}')^2\right)\right]$$

and

$$\frac{1}{\ell_c} = \frac{\omega_p^2\,\nu_c}{(\omega^2 + \nu_c^2)c}\,.$$

5.2. Representation of Correlation Function

In order to make a reasonable choice of the correlation function $g(R)$, we realize that it has to satisfy a few requirements:[19]

(1) $g(R) \to 0$ as $R \to \infty$,

(2) $\frac{d^2g(R)}{dR^2}$ preferably negative and finite to give a decreasing function.

In addition, from Chapter 3 we know that the Fourier transformed function $\sigma_g(k)$ also has to satisfy the following conditions:

(1) $\sigma_g(k) \propto k^{-\frac{11}{3}}$, $\quad k_0 \ll k \ll k_d$;

(2) $\sigma_g(k) \propto e^{-\frac{k^2}{k_1}}$, $\quad k \gg k_d$;

(3) $\sigma_g(k)$ finite as $k \to 0$,

where $k_0 \sim \frac{1}{r_s}$, $k_d \sim \left(\frac{\epsilon^3}{\epsilon}\right)^{\frac{1}{4}}$, and k_1 is constant. The most common choice of correlation functions is the exponential function $e^{-\frac{r}{a}}$ and the Gaussian function $e^{-(r^2/a^2)}$. The Fourier transformed functions are $1/(a^2 + k^2)^2$ and $e^{-a^2k^2}$, respectively. Neither of them satisfy the $k^{-11/3}$ law. Tatarski[20] suggested a model for the correlation function in terms of the Hankel function $\mathcal{K}$ of imaginary arguments that would satisfy the requirements of $g(R)$; but unfortunately the Fourier transformed spectral function does not have an exponential range for large k. Later Shkarofsky[19] proposed an improved correlation function

$$g(R) = \frac{[k_0(R^2 + r_0^2)^{\frac{1}{2}}]^{\frac{\mu-1}{2}} \mathcal{K}_{\frac{\mu-1}{2}}[k_0(R^2 + r_0^2)^{\frac{1}{2}}]}{(k_0 r_0)^{\frac{\mu-1}{2}} \mathcal{K}_{\frac{\mu-1}{2}}[k_0 r_0]} . \quad (33)$$

The corresponding $\sigma_g(k)$ is

$$\sigma_g(k) = \frac{(k_0 r_0)^{\mu-1}[r_0(k^2+k_0^2)^{\frac{1}{2}}]^{-\frac{\mu+2}{2}} \mathcal{K}_{\frac{\mu+2}{2}}[r_0(k^2+k_0^2)^{\frac{1}{2}}] r_0^3 (2\pi)^{3/2}}{(k_0 r_0)^{\frac{\mu-1}{2}} \mathcal{K}_{\frac{\mu-1}{2}}[k_0 r_0]} . \quad (34)$$

Both of them satisfy all the requirements listed above. The general feature of $\sigma_g(k)$ is to be peaked at $k = k_0$. When $\frac{1}{r_0}(=k_d) > k > k_0$, it goes like $k^{-(\mu+2)}$; so by taking $\mu = \frac{2}{3}$, $k \to k^{-11/3}$, when $k > k_d$, it decreases as $e^{-\frac{k^2}{\text{const.}}}$.

In our work we adopted Shkarofsky's expression and chose $\omega_{in} = 8.73 \cdot 10^8$ rad/sec and $k_{in} = 2.911 \times 10^{-2}$ cm^{-1}. The parameter r_0 was taken as 10 cm, which gave $k_d \sim 10^{-1} > k$ (in scattering k will range from 0 to $2k_{in}$). The other parameter k_0 should be $\sim r_s^{-1}$. But in general the size of the plasma is much greater than the wavelength k^{-1}, so usually $k \gg k_0$. This will cause $\sigma_g(k)$ to have a sharp peak at k_0. In our problem we need to Fourier analyze $\sigma_g(k)$; the sharp peak thus induces the convergence problem. To solve the difficulty, we recall that in the transport equation the scattering matrix $\underset{\sim}{M}$ may be divided into $\underset{\sim}{M} = \underset{\sim}{M}_s + \underset{\sim}{M}_c$ according to the k-space, which is either small or comparable to the incident wave vector k_{in}. The smaller k-space part corresponds to forward scattering. The larger k-space, which is comparable to k_{in}, corresponds to large angle and backscattering. It was pointed out by Watson[21] that if we define

$$\frac{\underset{\sim}{I}(\hat{p})}{\ell_s} = \int \underset{\sim}{M}_s(\hat{p}',\hat{p})\cdot I(\hat{p})\, d\Omega_{\hat{p}'},$$

then

$$\frac{\partial}{\partial s}\underset{\sim}{I}(\hat{p}) + \left(\frac{1}{\ell} - \frac{1}{\ell_s}\right)\underset{\sim}{I}(\hat{p}) = \int \underset{\sim}{M}_L(\hat{p},\hat{p}')\cdot\underset{\sim}{I}(\hat{p}')\, d\Omega_{\hat{p}'}.$$

We may say that the small k-space contributes nothing to the transport phenomena. Thus we can approximately set $k_0 \sim \frac{1}{2} k_{in}$ in our $\sigma_g(k)$ function. In this approximation, the k-vector, which lies between $k_0 = \frac{1}{2} k_{in}$ and $k_d = \frac{1}{r_0}$, still obeys the $k^{-11/3}$ law, just as $k_0 = \frac{1}{r_s}$, except that there is a constant factor of difference. Since the strength of the turbulence is a parameter that we have to set in front of $\sigma_g(k)$, we can easily adopt the $k_0 = \frac{1}{2} k$ approximation by multiplying the function by a constant correction factor. The solution $\underset{\sim}{I}$ was checked, and it turned out that the $k_0 = \frac{1}{2} k_{in}$ approximation was accurate to a few percent.

5.3. General Feature of the Scattered Signal

Now let us come to the general feature of the back-scattering wave in slab geometry. In a homogeneous medium, the scattering mean free path is constant. The essential parameters that will change the characteristics of the scattered signal are L_s and ξ, which are defined as follows:

$$L_s = \frac{D}{\ell} \tag{35}$$

$$\xi = \frac{\frac{1}{\ell_t}}{\frac{1}{\ell_c}}, \tag{36}$$

Where D is the slab thickness. We can recognize the significance of the two parameters through the integral representation of the transport equation

$$\underset{\sim}{I}(X,\hat{p}) = \underset{\sim}{I}_0\, e^{-\int_{k_{in}} \frac{ds}{\ell}}\, \delta_{\hat{k}_{in},\hat{p}} + \int_{-\hat{p}} ds(Z) \exp\left(-\int_Z^X \frac{ds}{\ell}\right)$$

$$\cdot \int d\Omega_{\hat{p}'}\, \underset{\sim}{M}(\hat{p},\hat{p}',X)\cdot\underset{\sim}{I}(X,\hat{p}'). \tag{14}$$

If we iterate the equation once, it becomes

$$\underset{\sim}{I}_{DWBA}(\hat{p}) = \underset{\sim}{I}_0\, e^{-\int_{k_{in}} \frac{ds}{\ell}}\, \delta_{\hat{k}_{in},\hat{p}} + \int_{-\hat{p}} ds(Z)\exp\left(-\int_{\hat{p}}^{X} \frac{ds'}{\ell}\right)$$

$$\times\ \underset{\sim}{M}(\hat{p},\hat{k}_{in})\cdot\underset{\sim}{I}_0 \exp\left(-\int_{\hat{k}_{in}} \frac{ds''}{\ell}\right), \tag{37}$$

which is called the Distorted Wave Born Approximation (DWBA). Noitce that only the coherent wave has been considered. Moreover, when $\ell \to \infty$, there is effectively no loss in the incident beam; the Born Approximation (BA) then is valid. We will have for a slab of thickness D

$$\underset{\sim}{I}_{BA}(\hat{p}) = \underset{\sim}{I}_0\, \delta_{\hat{k}_{in},\hat{p}} + \frac{D}{\mu_p}\underset{\sim}{M}(\hat{p},\hat{k}_{in})\cdot\underset{\sim}{I}_0. \tag{38}$$

The factor $\frac{1}{\mu_p}$ in the above equation takes care of the oblique propagation of the wave in the slab, in which case the pathway in the $\hat{p}$ direction is $\frac{D}{\mu_p}$.

The general feature of the cross section of the parallel polarization $\sigma_{||}$ for multiple scattering (MS), DWBA, and BA are plotted in Figs. 1 and 2 as a function of L_s. Figure 1 is for backscattering, i.e., $\theta = \pi - \theta_{\hat{k}_{in}}$ and $\phi = \pi$ (set $\phi_{\hat{k}_{in}} = 0$). Figure 2 is for bistatic scattering, $\theta = \pi - \theta_{\hat{k}_{in}}$ and $\phi = 0$. In the region of $L_s \ll 1$ (equivalent to the case of $\ell \to \infty$ for D finite), the three curves coincide. But in the region of $L_s \gtrsim 1$, both DWBA and MS level off while BA goes up as a straight line. The upper limit of L_s for which BA is valid may be obtained by the following argument.

A necessary condition for BA to be valid is that the angular deviation of the beam across the whole slab be much smaller than the angle difference α between the incident beam and the surface of the slab.[22] The deviation of angle per unit length can be defined as

$$\overline{\theta^2} \sim \int \theta^2 \sigma_g(\theta)(1 + \cos^2\theta)\, d\Omega_\theta .$$

Recalling that

$$\frac{1}{\ell} \sim \int \sigma_g(\theta)(1 + \cos^2\theta)\, d\Omega_\theta ,$$

and because in our problem $\sigma_g(\theta)$ is a smooth function of θ, we may say that the angular deviation is one radian when the

beam goes through the distance ℓ. The condition $\alpha^2 \gg \overline{\theta^2}$ is equivalent to

$$\alpha^2 \gg \frac{R}{\ell} = \frac{D}{(\sin\alpha)\ell} = \frac{L_s}{\sin\alpha} ; \qquad (39)$$

so in order to have BA valid,

$$L_s \ll \alpha^2 \sin\alpha .$$

In our calculation we have $\alpha \sim 20^\circ$; thus $L_s \ll 4 \times 10^{-2}$, which is verified and can be seen in Figs. 3 and 4.

Neglect of the scattering of the incoherent wave in both BA and DWBA causes changes in $\sigma_{||}$ as well as in the cross section of cross-polarization $\sigma_\perp$ in MS. It is quite obvious that the magnitude of the changes will depend on the parameter ξ because ξ is the ratio of the loss due to scattering to that due to collision. When $\xi \ll 1$, the collision loss is dominant and the contribution from the scattering of incoherent wave is relatively small; thus the difference between MS and DWBA will not be significant. But as ξ increases, the difference will increase also. This particular phenomena can be seen even more clearly with $\sigma_\perp$. For backscattering, both BA and DWBA have $\sigma_\perp = 0$ for all ξ and all L_s. But in MS, $\sigma_\perp$ depends strongly on ξ, as we see by comparing Figs. 3 and 4. Notice that we have also plotted the curve for $\phi = 0$. It is interesting to see that $\sigma_\perp$ in BA and DWBA are also zero in this case. And the slope of $\sigma_\perp(\phi = 0)$ on L_s is different from that of $\sigma_{||}(\phi = 0)$.

The absolute variation of $\sigma_{||}$ and $\sigma_{\perp}$ with ξ are plotted in Fig. 5. They are drawn according to four different slab thicknesses D. The ξ was varied by changing the collision frequency ν_c but keeping the strength of the turbulence $\frac{\langle \delta\rho \rangle}{\bar{\rho}}$ constant. Thus when ξ varies, the scattering mean free path ℓ also varies. In the lowest curve, where $L_s \ll 1$ for all ξ, $\sigma_{||}$ remains the same for all ξ, which is expected because BA is valid here. So even though ℓ changes, it does not affect the results at all. However, $\sigma_{\perp}$ varies a great deal as ξ increases. This is because the cross polarization comes from the scattering of incoherent waves; so it increases very fast when the scattering effect becomes significant compared with the collision loss. When D increases upward, it gradually passes the region where BA is valid; we can see the variation of both $\sigma_{||}$ and $\sigma_{\perp}$ when ξ varies. When we read the top two sets of curves, for the case of $\xi \sim 10^{-3}$, L_s is already $\gtrsim 1$; so both $\sigma_{\perp}$ and $\sigma_{||}$ keep the same magnitude, as we have pointed out before.

We also varied the incident angle α of the beam with respect to the surface of the slab $(\alpha = \frac{\pi}{2} - \theta)$. The relative variation for $\sigma_{||}$ and $\sigma_{\perp}$ at both $\phi = 0$ and $\phi = \pi$ are plotted in Fig. 6 as a function of $\mu = \sin\alpha$. The next three figures are drawn for different values of L_s. When $L_s \sim 10^{-7}$, MS and BA coincides for parallel polarization cross section $\sigma_{||}$. The variation of $\sigma_{||}(\phi = \pi)$ should be as $\propto \sigma_g(2k_{in}) \frac{D}{\mu}$, which is a hyperbolic function of μ. But for $\sigma_{||}(\phi = 0)$, it is a bistatic scattering, and should vary as $\sigma_g[2k_{in}(1 - \mu^2)^{\frac{1}{2}}] \frac{D}{\mu}$.

The angle dependence of the spectral function σ_g is quite obviously shown by the curves. When L_s reaches 10^{-1}, the difference between MS and BA can be seen; when L_s gets to ~ 1, the distinction between the two is rather striking.

Before we conclude this chapter, we want to emphasize one point--that the correlation function we have used is just one example that fits some peculiar properties of a turbulent fluid plasma--so that we may compare our approximation with some experiments. The general feature of the backscattering power from the slab geometry actually is independent of whatever the correlation function σ_g is, because they only depend on the two parameters L_s and ξ, and not on σ_g.

6. APPLICATION TO IONOSPHERIC AURORA

The ionospheric polar aurora occurs at about 70° latitude at a height around 110 km north hemisphere. It has been found that the backscattered radar signal is much enhanced when the aurora occurs. Farley[23] in 1963 claimed that the aurora was caused by ion-acoustic instability. Later, the experiments[24] showed that during the aurora, the disturbance seemed to transfer from one k-vector to other k-vectors. There is possibly turbulence in the medium.

When we look into possible causes of the turbulence, we must remember that there are particles precipitating from outer space into the ionosphere, that there are winds blowing the medium around, and that there also are electric and magnetic fields present. We also remember that in the E-region the density[25] of neutrals is 10^{11} to 10^{13} per cm^3, while the density of the electrons and ions is 10^4 to 10^5 per cm^3. The collisional frequency between electrons and neutrals is 10^4 to 10^5/sec, while that between electrons and ions is 10^2 to 10^3/sec. The collisions between the electrons and neutrals are apparently very important. On the other hand, the surrounding magnetic and electric fields cannot be neglected either. Our transport equation now serves the purpose of finding out by which mechanism the radar signal is scattered, by comparing the experimental results with the theoretical calculation of some particular models we assumed.

In order to find out whether the electrons will follow the neutrals or not, we consider that the electrons usually follow the ions, while the equation of motion for the ions in

quasi-equilibrium is

$$q_i\left(\underset{\sim}{E} + \frac{\underset{\sim}{v}_i}{c}\right)\underset{\sim}{B} \sim \nu_{in}(\underset{\sim}{v}_i - \underset{\sim}{v}_n)\, m_i \,, \tag{40}$$

where $\underset{\sim}{E}$ and $\underset{\sim}{B}$ are the external electric and magnetic fields; q_i, v_i, m_i are the charge, mean velocity, and mass of the ions; v_n is the mean velocity of the neutrals; and ν_{in} is the collision frequency between ions and neutrals,

$$\nu_{in} \sim 2.5 \times 10^{-15}\, v_i\, \rho_n \tag{41}$$

with ρ_n as the density of the neutrals. If the ions will follow the neutrals, we should have

$$\frac{|\underset{\sim}{v}_i - \underset{\sim}{v}_n|}{|\underset{\sim}{v}_n|} \ll 1$$

or

$$\left|\frac{q_i}{m_i}\left(\underset{\sim}{E} + \frac{\underset{\sim}{v}_i}{c} \times \underset{\sim}{B}\right)\right| \ll |\nu_{in}\, \underset{\sim}{v}_n| \,. \tag{42}$$

During the aurora, $E \sim 10^{-4}$ volt/cm;[26] and assuming $v_i \sim v_n \ll c$, we may neglect the contribution from the B field on the left-hand side of (42). Substituting Eq. (41) into (42), taking $\rho_n \sim 10^{13}$, we obtain

$$v_n^2 \gg 4 \times 10^{10} (\text{cm-sec})^2 \,. \tag{43}$$

So if the velocity of the neutrals is high enough that condition (43) can be satisfied, the electrons will follow the neutrals.

It was claimed[27] recently that it might be possible to have turbulent fluid motion for the neutrals in the E-region.

In that case, some of our calculations done in the previous chapters for the turbulent plasma are applicable, except that in the presence of magnetic field the scattering matrix for a single electron becomes

$$\underset{\sim}{f} = \frac{-e^2}{mc^2}\begin{bmatrix} \frac{1}{1-\lambda^2} & i\frac{\lambda}{1-\lambda^2} & 0 \\ -i\frac{\lambda}{1-\lambda^2} & \frac{1}{1-\lambda^2} & 0 \\ 0 & 0 & 1 \end{bmatrix},$$

where $\lambda = \frac{\Omega_e}{\omega}$, Ω_e is the cyclotron frequency for the electron, and ω is the incident wave frequency. In the backscattered radar experiments, the radio frequencies are higher than 10^8 Hz, and $\Omega_e \sim 10^6$-10^7 Hz. So $\lambda \ll 1$ and $\underset{\sim}{f} \sim f_0 \underset{\sim}{1}$, just as we had before. Thus we may use the transport equation derived earlier practically without any change. However, we have to notice that the isotropic correlation function used previously is not applicable anymore because the magnetic field will bind the electrons around it by cyclotron resonance so that the diffusion coefficient of electrons perpendicular to the field will be much smaller than that parallel to the field. Before we solve the transport equation, let us check if the Born approximation is applicable in this problem. If it is applicable, the wave is scattered only once. Whether the spectral function is isotropic or nonisotropic does not matter; after all, only $\sigma_g(2k_{in})$ needs to be considered.

In order to find out whether the Born approximation is valid or not, we need to know the scattering mean free path ℓ, so that we may make comparisons with the slab thickness of the E-region. In the calculation of ℓ, we derived the value for the strength of turbulence from the measurments by Chesnut et al.[28] at Homer, Alaska, in 1967. They used a 20-m parabolic antenna to detect the backscattered power of the radio signal that was sent up to the E-region during the aurora. Six frequencies ranging from 50 MHz to 3000 MHz could be operated at the same time in the Homer radar. Three sets of data taken for four frequencies 139 MHz, 398 MHz, 850 MHz, and 1210 MHz during different auroras are drawn in Fig. 10. For each aurora, we fix the strength of turbulence by fitting the data of one particular frequency. It was found that the collisional loss is the main absorption. When we took $\ell \sim \ell_c$, it turned out that among the four frequencies, only the larger two are in the region where BA is valid. We took the slab thickness to be 60 Km and $r_0 = 10$ cm.[29] The comparison between the experimental cross section and the theoretical calculation in BA is shown in Fig. 10.

The fitting for the larger two frequencies looks pretty good. But for the smaller two, there is quite a discrepancy. On one hand, it is sort of expected, because multiple scattering causes levelling off of the cross section when BA is not applicable. On the other hand, it is doubtful whether the multiple scattering will lower the cross section to $\approx$10dB from the BA calculation because the L_s for the smaller two frequencies, although it does not satisfy the $L_s \ll \alpha^2 \sin\alpha (\sim 4 \times 10^{-2})$

requirement, is of the order of 10^{-2}. From our experience in calculation, there is some bending of MS from BA, but the difference between the two is quite small for $L_s \sim 10^{-2}$. However, there may be striking differences between the results of the isotropic spectral function and the anistotropic one, even though the collisional loss dominates. First of all, we no longer can employ the Fourier analysis method to separate the ϕ-angle dependence from the θ-angle dependence in our transport equation. Solving the whole transport equation of the anisotropic spectral function was not easy at all. We thus will reserve our comments on the cross section for the two smaller frequencies until further investigation is made.

If the turbulent fluid model is true--at least for the frequencies 850 MHz and 1210 MHz it works fine--we need to explain another important experimental result, which is described in the following. In the experiments,[28] it was found that during the aurora the radar beam has to be almost perpendicular to the magnetic field lines. If the beam direction is 3° to 5° away from the perpendicular, the signal power drops down 10 to 20 dB. This striking phenomenon is usually called the aspect sensitivity.

When we take the magnetic field into account, not only are the diffusion coefficients $\mathscr{D}_\perp$ and $\mathscr{D}_{||}$ different, but also the velocity components of the electrons $v_\perp$ and $v_{||}$ are not the same. It was found[29] that

$$v_{||} = (v_n)_{||}$$

$$v_\perp = \frac{(v_n)_\perp \nu_c}{(\nu_c^2 + \Omega_e^2)^{\frac{1}{2}}} ,$$

where $(v_n)_{||}$ and $(v_n)_\perp$ are the velocity components for neutral particles. In the E-region, $\nu_c \sim 10^5$ sec^{-1} and $\Omega_e \sim 10^7$ sec^{-1}, so

$$v_\perp \cong (v_n)_\perp \cdot 10^{-2} .$$

In the ionosphere, the neutrals are isotropic, so the magnitude of v_n is always the same. But for electrons moving at angle β with respect to the $\underset{\sim}{B}$ line, its magntidue will be

$$\begin{aligned} v(\beta) &= (v_\perp^2 + v_{||}^2)^{\frac{1}{2}} \\ &= [(v_n(\sin\beta)\cdot 10^{-2})^2 + (v_n \cos\beta)^2]^{\frac{1}{2}} \\ &= \frac{v_n}{100}(\sin^2\beta + 10^4 \cos^2\beta)^{\frac{1}{2}} . \end{aligned}$$

The parameter r_0 in $\sigma_g(k)$ is practically the characteristic size of the smallest eddy beyond which Kolmogoroff's law is not applicable. Let τ be the characteristic time such that

$$r_0 \sim v\tau .$$

We have found that $r_0 \sim 10$ cm[29] when $\beta = 90^\circ$; then

$$r_0(\beta) = \frac{v(\beta)}{v(90^\circ)} \cdot 10$$

when $\beta = 85^\circ$, r_0 turned out to be ~ 70 cm. Substituting these values into the expression for σ_g, we obtain

$$\sigma_g(2k_{in})\big|_{r_0=70} \Big/ \sigma_g(2k_{in})\big|_{r_0=10} \sim 10^{-1} ,$$

thus providing one possible explanation for the aspect sensitivity.

After going through the model of fluid turbulence, we may very well assume that the interaction between charged particles and the effect of outside fields overrule the collisional effect. If it is so, then the disturbance here is plasma turbulence. That is to say, it is due to the nonlinear effects between the particles and waves. We need to establish the energy spectrum of the system first, which may give us some information about the distribution of the electric field. Then we could find out the correlation of particles through Maxwell's equations. But the whole field of nonlinear effects in plasma is still in the pioneer stage. We hopefully will solve the problem in the near future to see if the plasma turbulence model holds true in the aurora or not.

7. BORN APPROXIMATION CONTROVERSY NEAR CRITICAL DENSITY

Recently, several works[30] on backscattering from turbulent plasma have been done. Whether or not the Born approximation is valid near the critical density becomes a point of much interest. (Here we are talking about $\sigma_{\parallel}$ of course; $\sigma_{\perp}$ in BA is not valid for any density.) From our previous analysis, we have seen that the features of the scattered signal depend on the two parameters L_s and ξ. Although our results were gained from slab geometry, we would expect the same features in cylindrical or rectangular geometry, which are the closest to that used in the experiments mentioned above. Our argument is that whether BA is valid or not does not depend on whether the density is near the critical value or not, but depends on whether under that circumstance the L_s is larger or smaller than the BA limit $\alpha^2 \sin\alpha$. We plotted in Fig. 11 a few curves at different slab thicknesses. When $D \sim 10^2$ cm, the L_s for $\rho = 10^4$ cm^{-3} to $\rho = 10^8$ cm^{-3} are all less than $\alpha^2 \sin\alpha$ ($\alpha = 20°$, $\rho_{crit} \sim 2 \times 10^8$ cm^{-3}). Thus the Born approximation should be valid. From our calculations, when ρ approaches 10^8 cm^{-3}, the curve of MS coincides with BA. As D becomes 5×10^5 cm, the L_s for $\rho = 10^7$ cm^{-3} to $\rho = 10^8$ cm^{-3} approach 1; thus the bending of MS is shown quite clearly as compared with BA.

It is quite possible that in the measurements by Granatstein et al.,[30] in an experiment of contained flow-discharge, even though $[\langle(\delta_\rho)^2\rangle]/(\rho_{crit})$ is only ~0.03. the size of the plasma is about the same as the scattering mean free path ℓ in that situation; so they found bending of $\sigma_{\parallel}$ near

the critical density. While in the experimental measurements by Guthart et al.[30] and Shkarofsky et al.--the former performed on a potassium seeded oxyacetylene flame and the latter obtained by a homodyne detection system--even though ρ_{crit} is approached, the relative strengths of the turbulence and the collision frequency in the medium have caused the size of the plasma to be small compared with their ℓ; so the Born approximation is still valid.

ACKNOWLEDGMENTS

The author is grateful to her advisor, Professor K. M. Watson for his guidance and support through the years. She is also thankful to Professor W. B. Kunkel for his encouragement and helpful discussions on this work.

FOOTNOTES AND REFERENCES

* This work was supported by the U. S. Atomic Energy Commission.

1. Booker, H. G. Radio Scattering in the Lower Ionosphere, J. Geophy. Res. 64, 2164-2177, 1959.

2. Ruffine, R. S., and D. A. deWolf, Cross-Polarized Electromagnetic Backscatter from Turbulent Plasmas, J. Geophy. Res. 70, 4313-4321, 1965.

3. Chandrasekhar, S., Radiative Transfer, Chapter 1, Clarendon Press, Oxford, 1950.

4. Feinstein, D. L., and V. L. Granatstein, Scalar Radiative Transport Model for Microwave Scattering From a Turbulent Plasma, Phys. Fluids 12, 2658 (1969).

5. Watson, K. M., Multiple Scattering of Electromagnetic Waves in an Underdense Plasma, J. Math. Phys. 10, 688 (1969).

6. Two other derivations of transport equations have been published by Yu. N. Barabanenkov and V. N. Finkel'berg, Zh. Eksp. Teop. Fiz. 53, 978 (1967) [Sov. Phys. JETP 26, 587 (1968)] and P. E. Stott, J. Phys. A (Proc. Phys. Soc.) Ser. 2, 1, 1496 (1968).

7. The transport equation for curved ray path was derived by C. Lau and K. M. Watson, J. Math. Phys. 11, 3125 (1970); Extension of transport equation to high-order approximation was done by C. Lau, Multiple Scattering of Electromagnetic Wave in an Underdense Plasma and the Radiation Transport Equation, Lawrence Radiation Laboratory Report UCRL-20689 April 1971 (Ph.D. Thesis).

8. McMaster, W. H., Polarization and Stokes Parameters, Am. J. Phys. 22, 351 (1954).

9. This section is an outline of Ref. 5; for details please go to the original paper.

10. This was kindly pointed out by Professor Wulf Kunkel.

11. Batchelor, G. K., The Theory of Homogeneous Turbulence, Chapter 6, Cambridge University Press, 1960.

12. Batchelor, G. K., Small-Scale Variation of Convected Quantities Like Temperature in Turbulent Fluid, J. Fluid Mech. 5, 113 (1959).

13. Tatarski, V. I., Wave Propagation in Turbulent Medium, Chapter 3, McGraw-Hill, 1961.

14. A similar argument for velocity field can be found in Chapter 5 of Ref. 11.

15. Davison, B., Neutron Transport Theory, Clarendon Press, London, 1957.

16. See Chapter 10 of Ref. 3.

17. See Chapter 2 of Ref. 3.

18. See Chapter 10 of Ref. 15.

19. Shkarofsky, I. P., Generalized Turbulence Space-Correlation and Wave-Number Spectrum-Function Pairs, Canad. J. Phys. 46, 2133 (1968).

20. Reference 13, p. 7.

21. Watson, K. M., Electromagnetic Wave Scattering Within a Plasma in the Transport Approximation, Phys. Fluids 13, 2514 (1970).

22. Salpeter, E. E. and Treiman, S. B., Backscatter of Electromagnetic Radiation from a Turbulent Plasma, J. Geophys. Res. 69, 869 (1964); Granatstein, V. L. and Buchsbaum, S. J., Microwave Scattering from Turbulent Plasma, Proceedings of Symposium on Turbulence of Fluids and Plasmas, 1968.

23. Farley, D. T., Jr., A Plasma Instability Resulting in Field-Aligned Irregularities in the Ionosphere, J. Geophys. Res. 68, 6083 (1963).

24. Chesnut, W. G., Low Frequency Waves and Irregularities in the Auroral Ionosphere as Determined by Radar Measurements, Low Frequency Waves and Irregularities in the Ionosphere, Springer-Verlag, N. Y. (1968).

25. Ginzburg, V. L., Propagation of Electromagnetic Wave in Plasma, Sec. 6, Gordon and Breach, 1961

26. Mozer, F. S. and Fahleson, U. V., Parallel and Perpendicular Electric Fields in an Aurora, Planet. and Space Sci. (GB) 18, 1536 (1970).

27. Tchen, C. M., Turbulence and Gravity Waves in the Upper Atmosphere, IDA Log No. HQ70-11468, 1970.

28. Chesnut, W. G., Hodges, J. C., and Leadabrand, R. L., Auroral Backscatter Wavelength Dependence Studies, Stanford Research Institute Report, Project 5535, 1968.

29. Booker, H. G., Turbulence in the Ionosphere with Application to Meteor Trails, Radio Star Scintillation, Auroral Radar Echoes, and Other Phenomena, J. Atmos. and Terres. Phys., A Special Supplement, 52, 1957.

30. Granatstein, V. L. and Buchsbaum, S. J., same as Ref. 22; Guthart, H. and Graf, K. A., Radio Science 2, 1099 (1970); Richard, C., Ghosh, A. K., Johnson, T. W., and Shkarofsky, I. P., Experimental Check of the Applicability of Single Born Scattering Theory Up To Critical Density Fluctuations, Phys.Fluids 14, 398 (1971).

TABLE I. The Matric Elements of M

$$M_{11} = \sigma_g[\sin\theta \sin\theta' + \cos\theta \cos\theta' \cos(\phi' - \phi)]^2$$

$$M_{12} = \sigma_g[\cos^2\theta \sin^2(\phi' - \phi)]$$

$$M_{13} = -\sigma_g \cos\theta \sin(\phi' - \phi)[\sin\theta \sin\theta' + \cos\theta \cos\theta' \cos(\phi' - \phi)]$$

$$M_{21} = \sigma_g[\cos^2\theta' \sin^2(\phi' - \phi)]$$

$$M_{22} = \sigma_g[\cos^2(\phi' - \phi)]$$

$$M_{23} = \sigma_g\left[\cos\theta' \sin[2(\phi' - \phi)]\right]/2$$

$$M_{31} = 2\,\sigma_g \cos\theta' \sin(\phi' - \phi)[\sin\theta \sin\theta' + \cos\theta \cos\theta' \cos(\phi' - \phi)]$$

$$M_{32} = -\sigma_g \cos\theta \sin[2(\phi' - \phi)]$$

$$M_{33} = \sigma_g[\cos\theta \cos\theta' \cos\left(2(\phi' - \phi)\right) + \sin\theta \sin\theta' \cos(\phi' - \phi)]$$

$$M_{44} = \sigma_g[\cos\theta \cos\theta' + \sin\theta \sin\theta' \cos(\phi' - \phi)]$$

$$M_{14} = M_{24} = M_{34} = M_{41} = M_{42} = M_{43} = 0.$$

TABLE II. The Gaussian Divisions and Gaussian Weights.

m = 1, N = 2	$\mu_{\pm1} = \pm0.5773503$	$a_1 = a_{-1} = 1$	
m = 2, N = 4	$\mu_{\pm1} = \pm0.3399810$	$a_1 = a_{-1} = 0.6521452$	
	$\mu_{\pm2} = \pm0.8611363$	$a_2 = a_{-2} = 0.3478548$	
m = 3, N = 6	$\mu_{\pm1} = \pm0.2386192$	$a_1 = a_{-1} = 0.4679139$	
	$\mu_{\pm2} = \pm0.6612094$	$a_2 = a_{-2} = 0.3607616$	
	$\mu_{\pm3} = \pm0.9324695$	$a_3 = a_{-3} = 0.1713245$	
m = 4, N = 8	$\mu_{\pm1} = \pm0.1834346$	$a_1 = a_{-1} = 0.3626838$	
	$\mu_{\pm2} = \pm0.5255324$	$a_2 = a_{-2} = 0.3137066$	
	$\mu_{\pm3} = \pm0.7966665$	$a_3 = a_{-3} = 0.2223810$	
	$\mu_{\pm4} = \pm0.9602899$	$a_4 = a_{-4} = 0.1012285$	

TABLE III. The Backscatter Transfer Matrix $\mathcal{J}$.

$$\mathcal{J}_{11} = T_{11} + \Delta T_{11}$$

$$\mathcal{J}_{12} = T_{12} + \frac{1}{2}\Delta T_{44} - \frac{1}{2}\Delta T_{33}$$

$$\mathcal{J}_{13} = T_{13} + \frac{1}{2}\Delta T_{13} - \frac{1}{4}\Delta T_{31}$$

$$\mathcal{J}_{21} = T_{21} + \frac{1}{2}\Delta T_{44} - \frac{1}{2}\Delta T_{33}$$

$$\mathcal{J}_{22} = T_{22} + \Delta T_{22}$$

$$\mathcal{J}_{23} = T_{23} + \frac{1}{2}\Delta T_{23} - \frac{1}{4}\Delta T_{32}$$

$$\mathcal{J}_{31} = T_{31} + \frac{1}{2}\Delta T_{31} - \Delta T_{13}$$

$$\mathcal{J}_{32} = T_{32} + \frac{1}{2}\Delta T_{32} - \Delta T_{23}$$

$$\mathcal{J}_{33} = T_{33} + \frac{1}{2}\Delta T_{33} + \frac{1}{2}\Delta T_{44} - \frac{1}{2}\Delta T_{21} - \frac{1}{2}\Delta T_{12}$$

$$\mathcal{J}_{44} = T_{44} + \frac{1}{2}\Delta T_{33} + \frac{1}{2}\Delta T_{44} + \frac{1}{2}\Delta T_{21} + \frac{1}{2}\Delta T_{12}$$

$$\mathcal{J}_{14} = \mathcal{J}_{24} = \mathcal{J}_{34} = \mathcal{J}_{41} = \mathcal{J}_{42} = \mathcal{J}_{43} = 0.$$

FIGURE CAPTIONS

Fig. 1. The parallel polarization cross section $\sigma_{||}$ calculated from the Born Approximation (BA), the Distorted Wave Born Approximation (DWBA), and the Multiple Scattering regime (MS) for backscattered signal at $\theta = \pi - \theta_{\hat{k}_{in}}$ and $\phi = \pi$ ($\phi_{\hat{k}_{in}} = 0$). L_s is the ratio of the slab thickness to the scattering mean free path.

Fig. 2. Parallel polarization cross section $\sigma_{||}$ for bistatic scattered signal at $\theta = \pi - \theta_{\hat{k}_{in}}$ and $\phi = 0$.

Fig. 3. Parallel polarization $\sigma_{||}$ and cross polarization $\sigma_{\perp}$ for both backscattered signal ($\phi = \pi$) and bistatic scattered signal ($\phi = 0$) vs L_s. We have ℓ_t as the scattering loss constant, ℓ_c the collisional absorption constant, ρ the electron density and $\langle \rho - \bar{\rho} \rangle / \bar{\rho}$ the strength of the turbulence in the medium.

Fig. 4. The ratio of the scattering loss to the collisional absorption was set at 2.3×10^{-3} to compare the cross sections with those shown in Fig. 3. The dotted lines are from the Born approximation, the solid lines are from the multiple scattering model.

Fig. 5. Variation of the cross sections of the backscatterd signal vs ξ, the ratio of the scattering loss to the collisional absorption.

Fig. 6. Illustrate the dependence of the cross sections on the incident angle α of the beam relative to the surface

of the slab. The coordinates μ is $\sin\alpha$, and $L_s \sim 10^{-2}$.

Fig. 7. Similar to Fig. 6 except that $L_s \sim 10^{-7}$. The Born approximation fits well for all μ's.

Fig. 8. Comparing with Fig. 7, the difference between the Born approximation and the multiple scattering starts to show when $L_s \sim 10^{-1}$.

Fig. 9. The general feature of the curves are different from thos shown in the previous three figures. For $L_s \sim 1.4$, only the multiple scattering model is valid.

Fig. 10. Comparison between the experimental measurements and the theoretical calculations for ionospherical aurora at frequencies 139 MHz, 398 MHz, 850 MHz, and 1210 MHz.

Fig. 11. To illustrate how the validity of the Born approximation near the critical density does not depend on the density ρ, but depends on L_s.

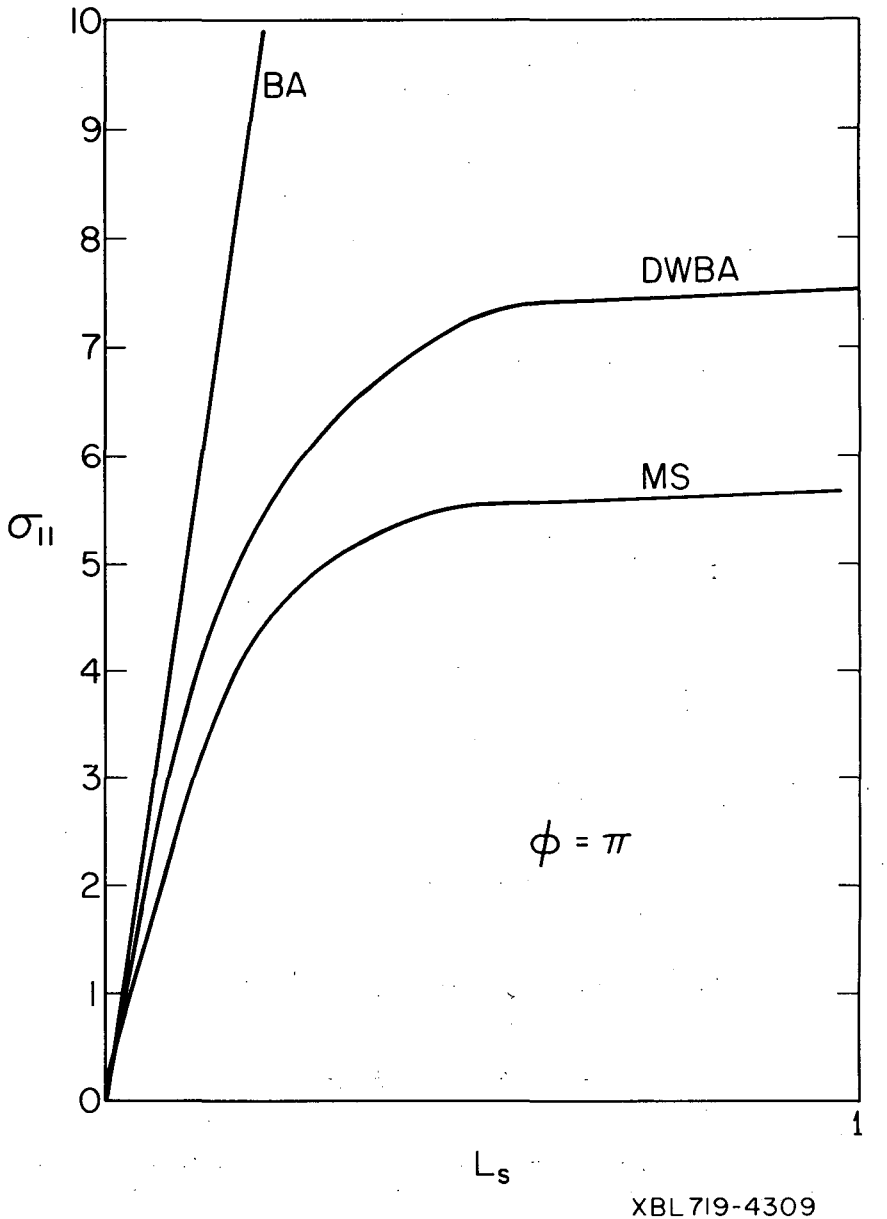

Fig. 1.

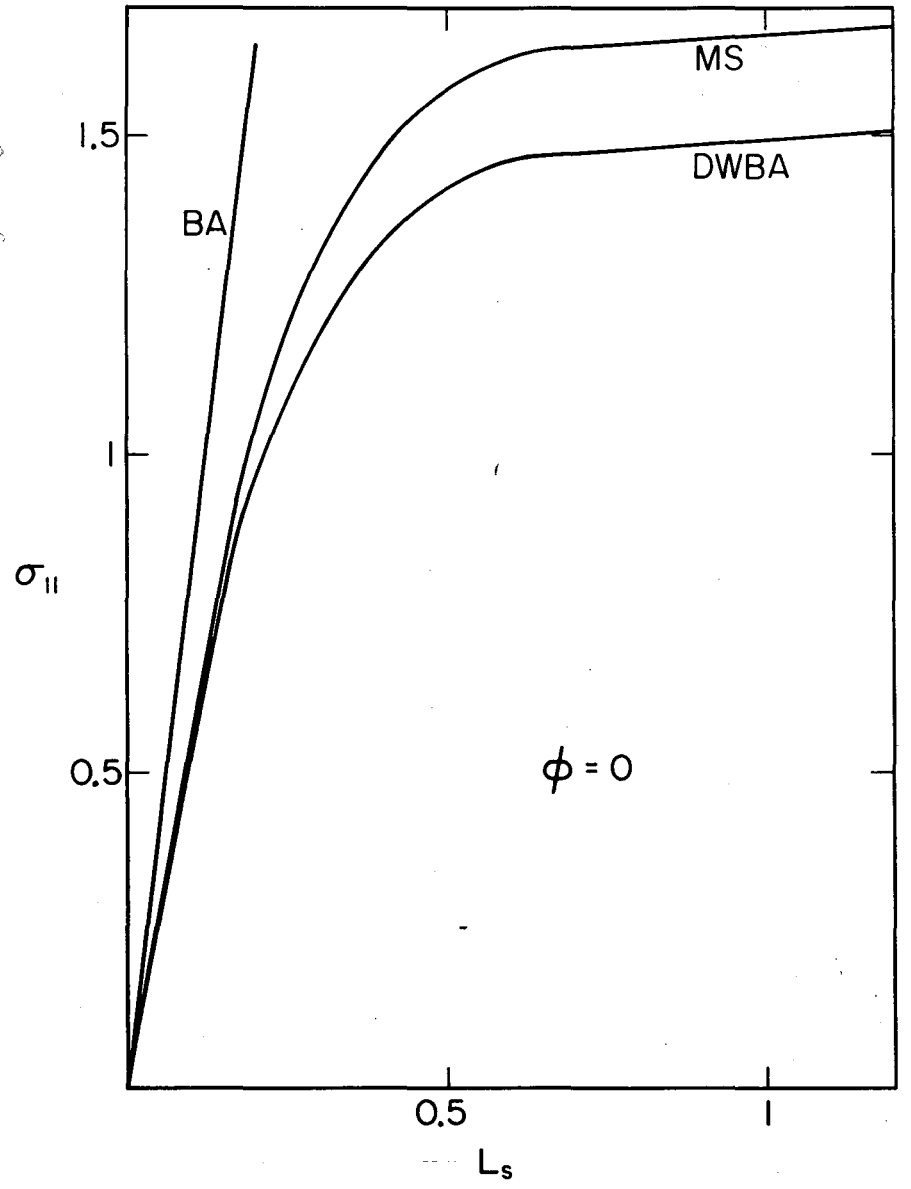
MS
DWBA
BA
1.5
1
0.5
σ_{11}
$\phi = 0$
0.5
1
L_s
XBL719-4324

Fig. 2.

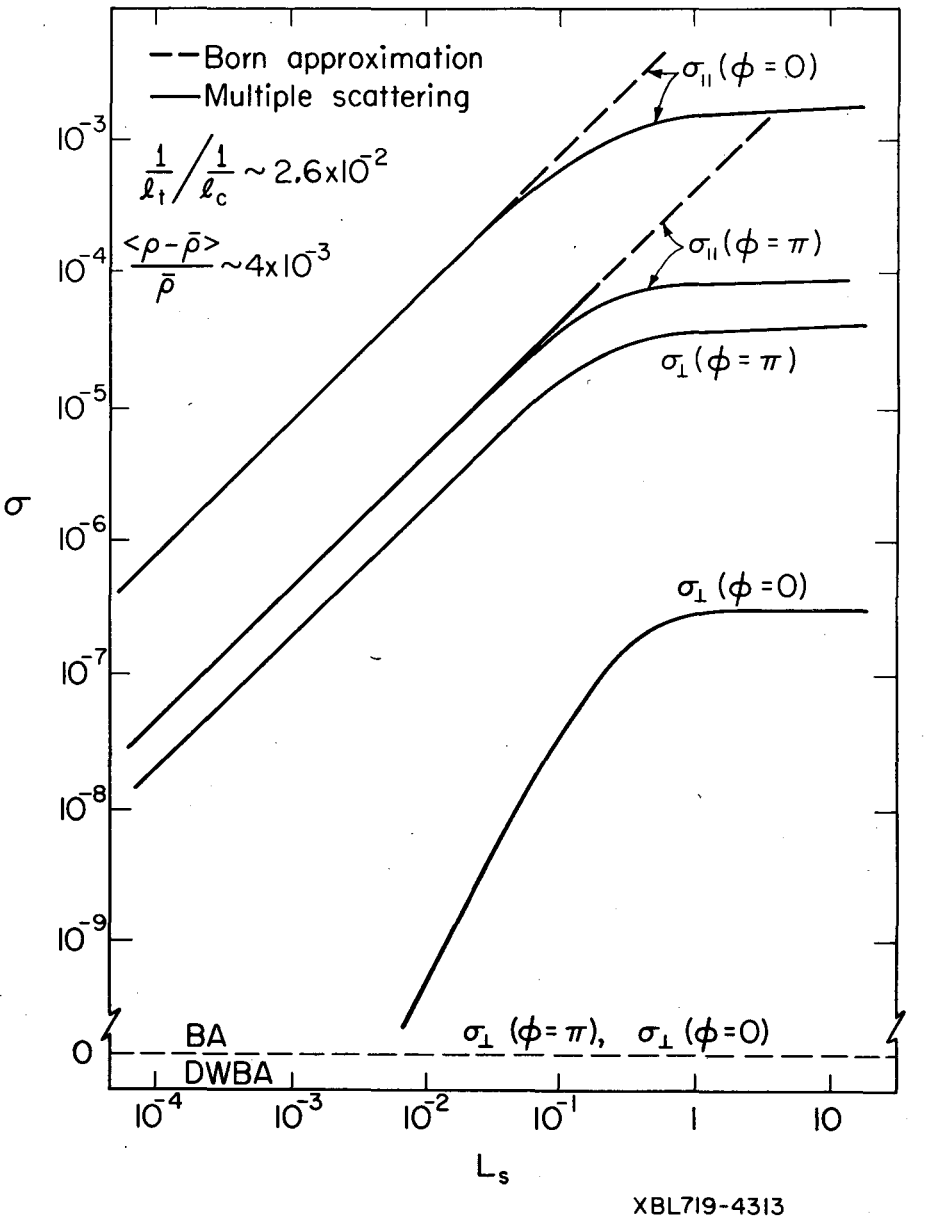
Born approximation
Multiple scattering
$\frac{1}{\ell_t} / \frac{1}{\ell_c} \sim 2.6 \times 10^{-2}$
$\frac{\langle \rho - \bar{\rho} \rangle}{\bar{\rho}} \sim 4 \times 10^{-3}$
$\sigma_{11}(\phi = 0)$
$\sigma_{11}(\phi = \pi)$
$\sigma_{\perp}(\phi = \pi)$
$\sigma_{\perp}(\phi = 0)$
σ
10^{-3}
10^{-4}
10^{-5}
10^{-6}
10^{-7}
10^{-8}
10^{-9}
0
BA
DWBA
$\sigma_{\perp}(\phi = \pi)$, $\sigma_{\perp}(\phi = 0)$
10^{-4}
10^{-3}
10^{-2}
10^{-1}
1
10
L_s
XBL719-4313

Fig. 3.

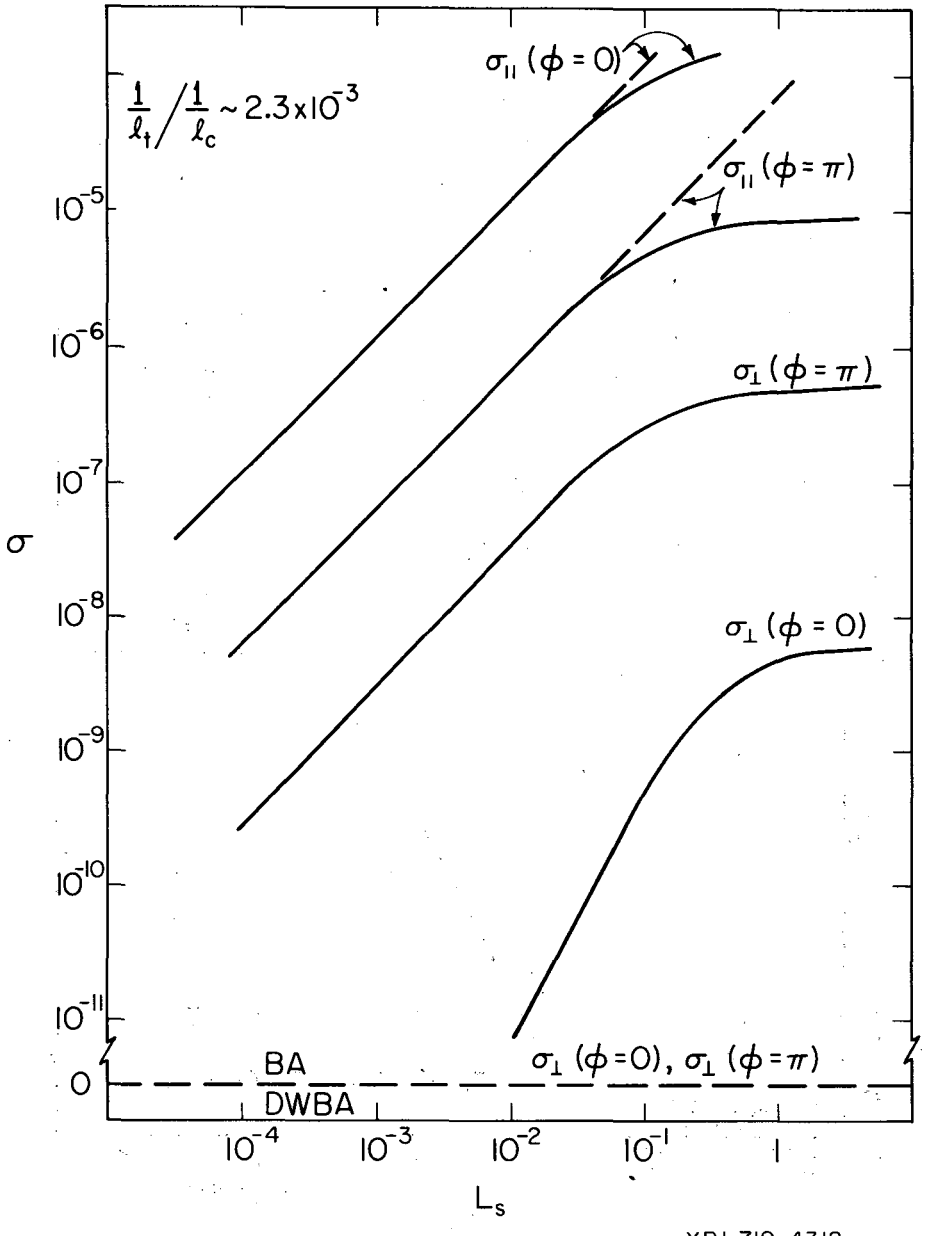

XBL719-4312

Fig. 4.

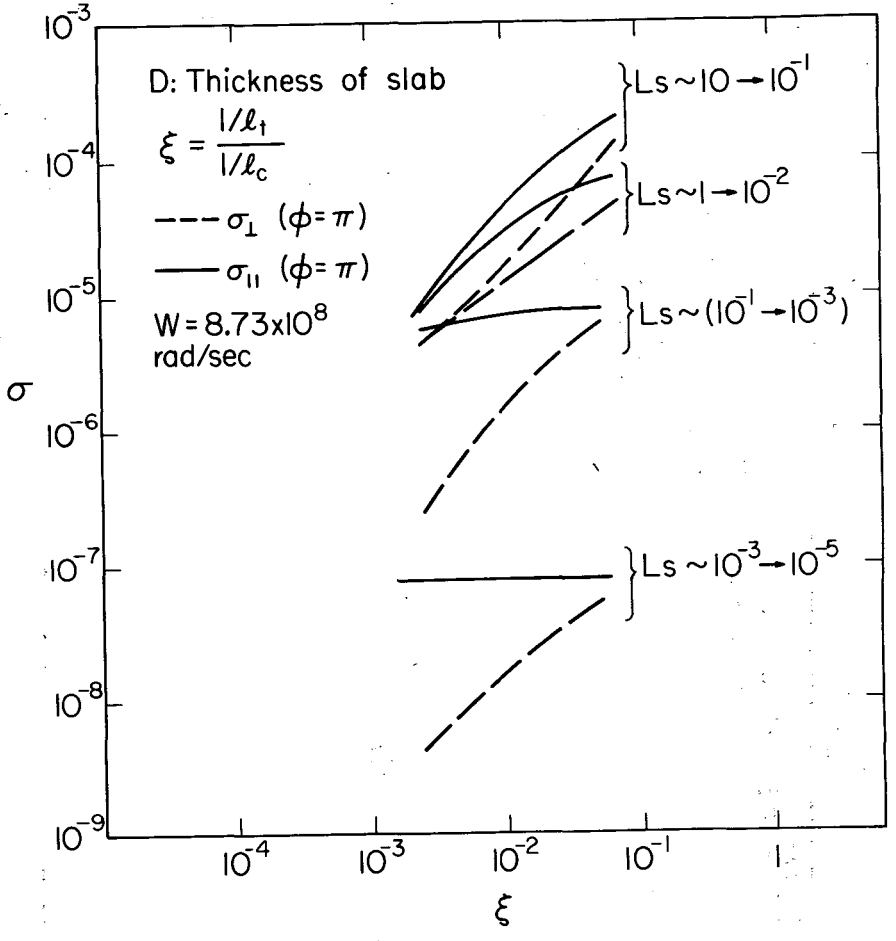

XBL719-4310

Fig. 5.

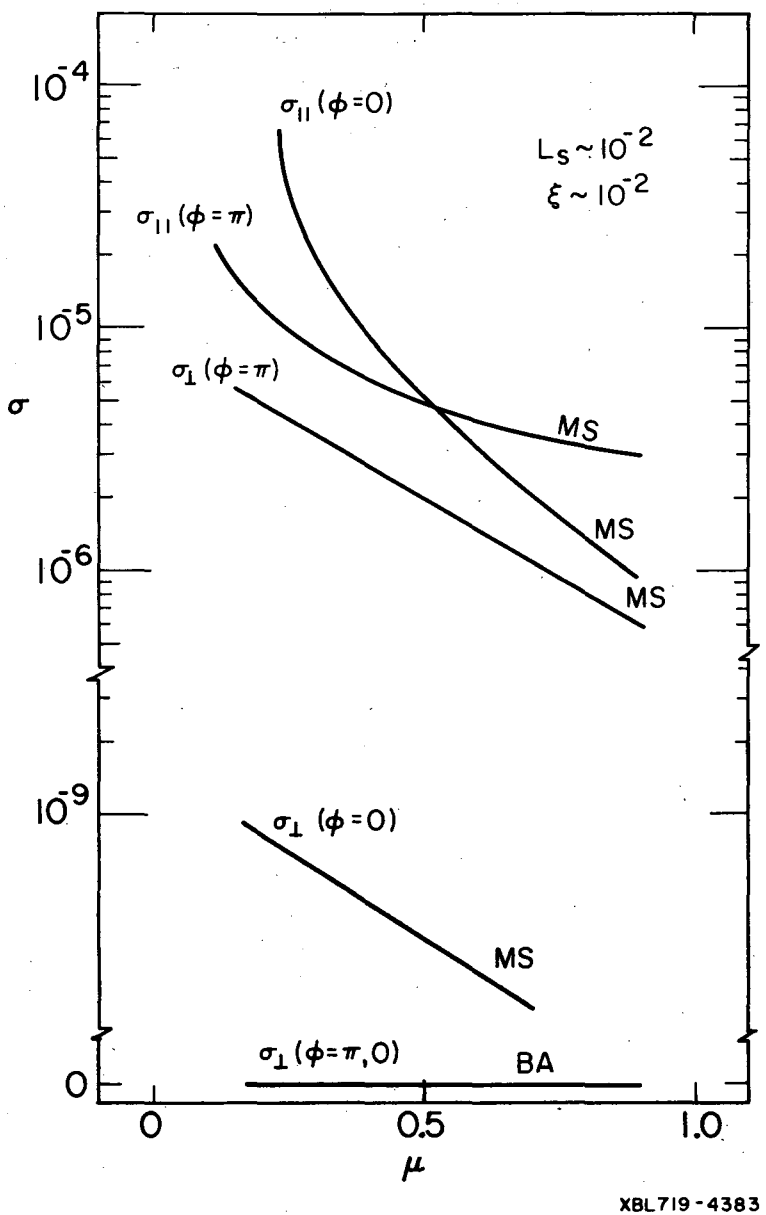
10^{-4}
10^{-5}
10^{-6}
10^{-9}
0
σ
$\sigma_{11}(\phi=0)$
$L_s \sim 10^{-2}$
$\xi \sim 10^{-2}$
$\sigma_{11}(\phi=\pi)$
$\sigma_\perp(\phi=\pi)$
MS
MS
MS
$\sigma_\perp(\phi=0)$
MS
$\sigma_\perp(\phi=\pi,0)$
BA
0
0.5
1.0
μ
XBL719-4383

Fig. 6.

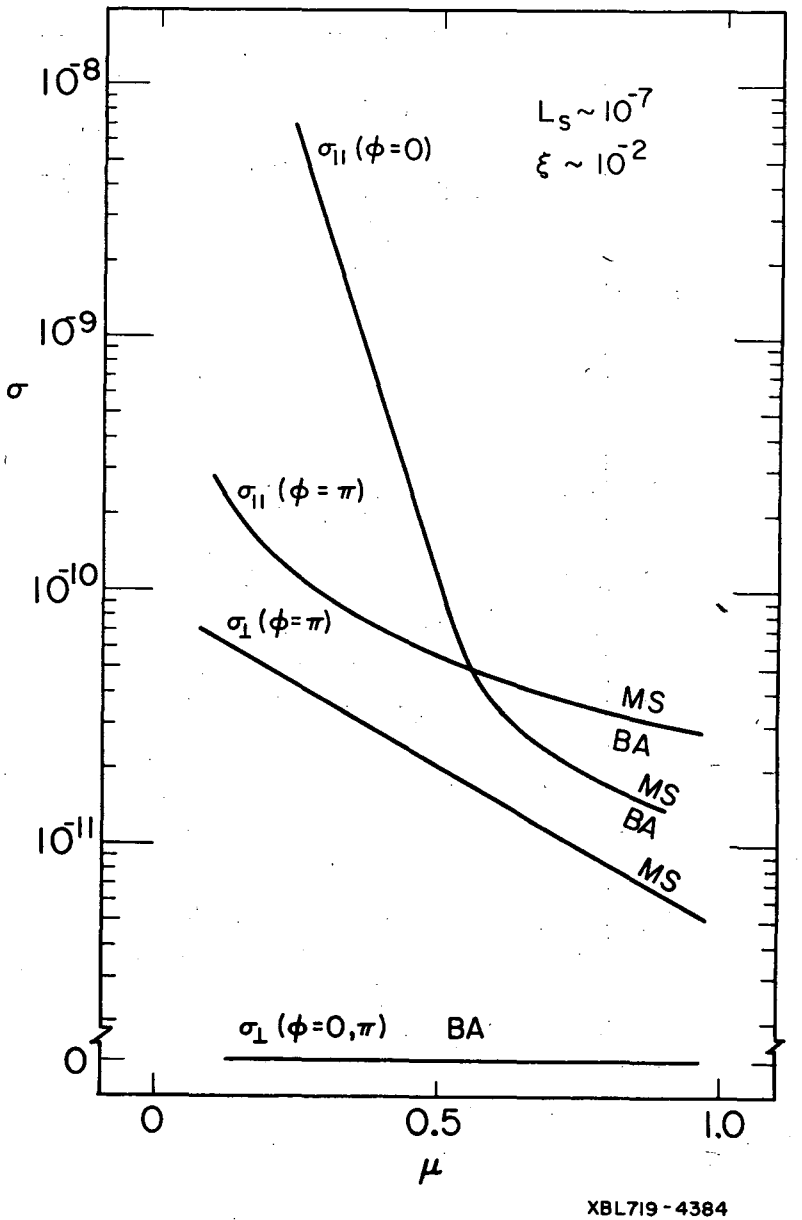
10^{-8}
10^{-9}
10^{-10}
10^{-11}
0
σ
$\sigma_{11}(\phi=0)$
$L_s \sim 10^{-7}$
$\xi \sim 10^{-2}$
$\sigma_{11}(\phi=\pi)$
$\sigma_\perp(\phi=\pi)$
MS
BA
MS
BA
MS
$\sigma_\perp(\phi=0,\pi)$
BA
0
0.5
1.0
μ
XBL719-4384

Fig. 7.

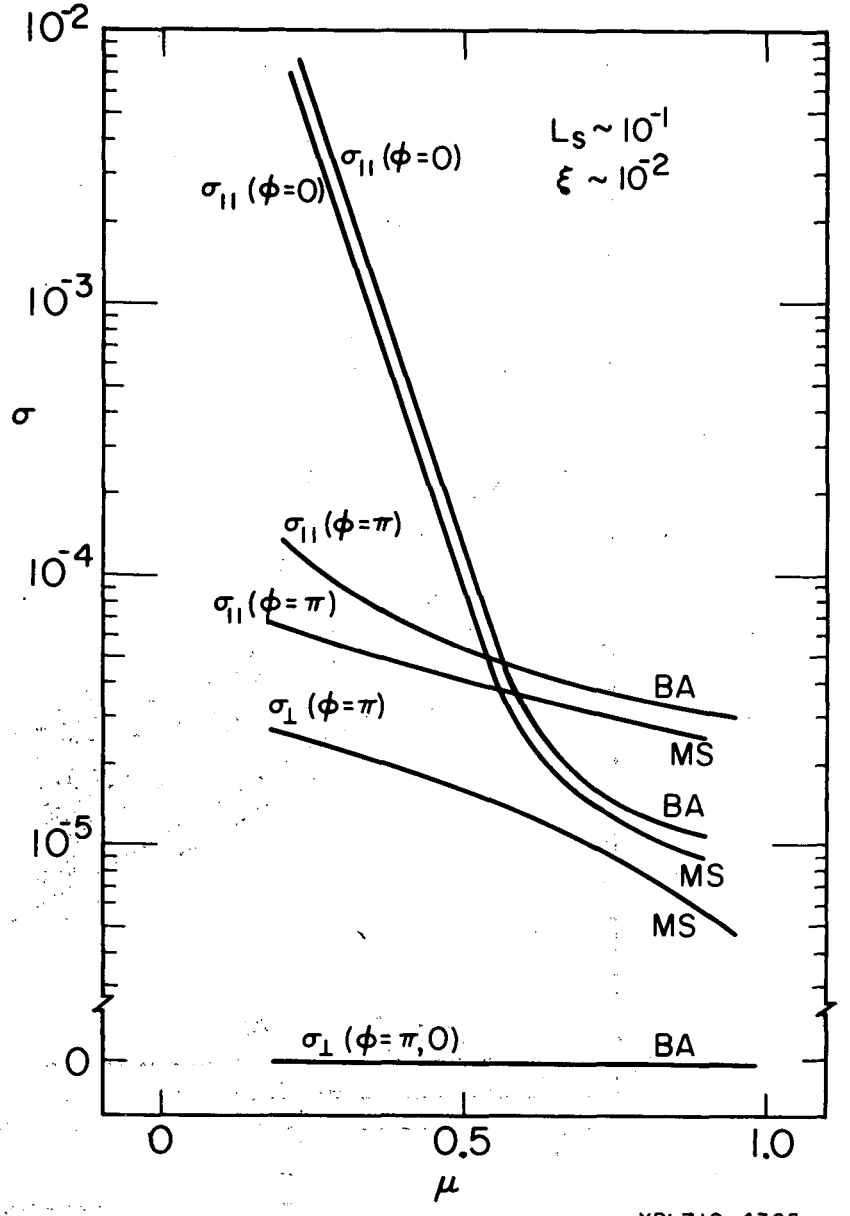
10^{-2}
10^{-3}
10^{-4}
10^{-5}
0
σ
$L_s \sim 10^{-1}$
$\xi \sim 10^{-2}$
$\sigma_{11}(\phi=0)$
$\sigma_{11}(\phi=0)$
$\sigma_{11}(\phi=\pi)$
$\sigma_{11}(\phi=\pi)$
$\sigma_\perp(\phi=\pi)$
$\sigma_\perp(\phi=\pi,0)$
BA
MS
BA
MS
MS
BA
0
0.5
1.0
μ
XBL719-4385

Fig. 8.

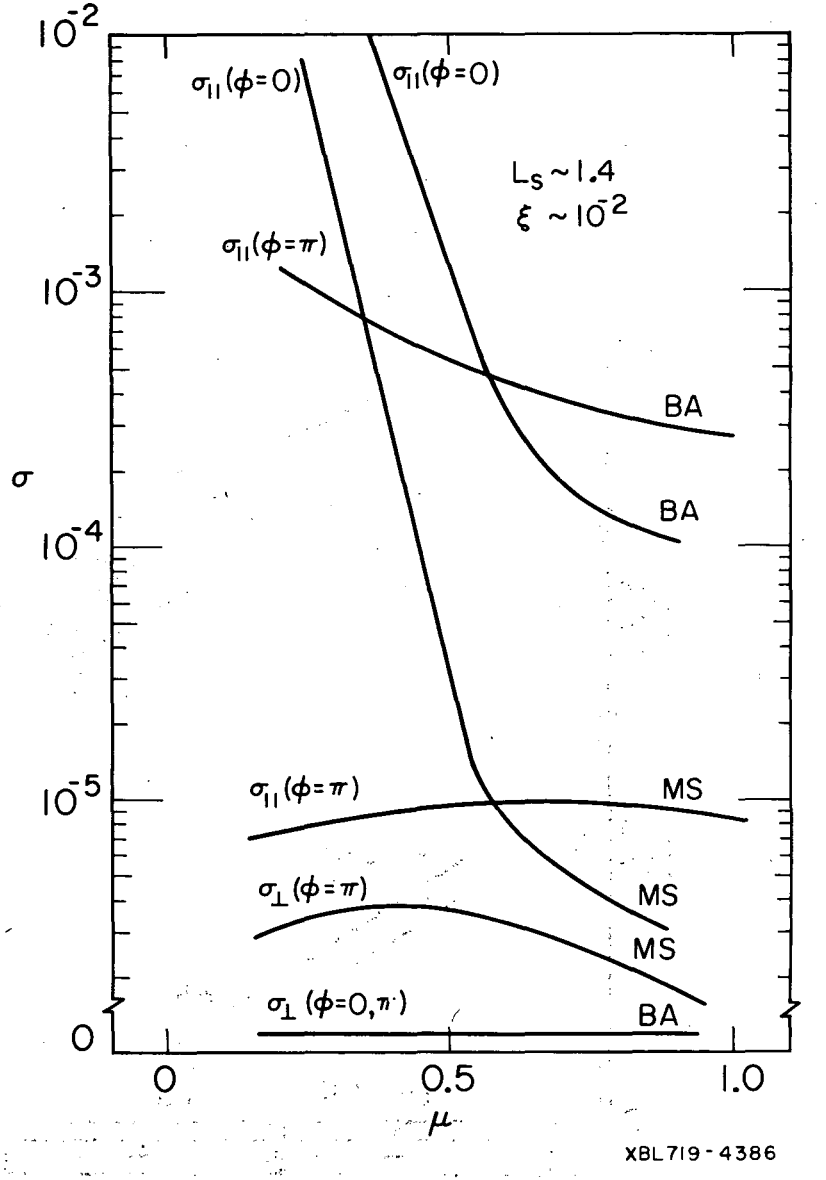
10^{-2}
10^{-3}
10^{-4}
10^{-5}
0
σ
$\sigma_{11}(\phi=0)$
$\sigma_{11}(\phi=0)$
$L_s \sim 1.4$
$\xi \sim 10^{-2}$
$\sigma_{11}(\phi=\pi)$
BA
BA
$\sigma_{11}(\phi=\pi)$
MS
$\sigma_\perp(\phi=\pi)$
MS
MS
$\sigma_\perp(\phi=0,\pi)$
BA
0
0.5
1.0
μ
XBL719-4386

Fig. 9.

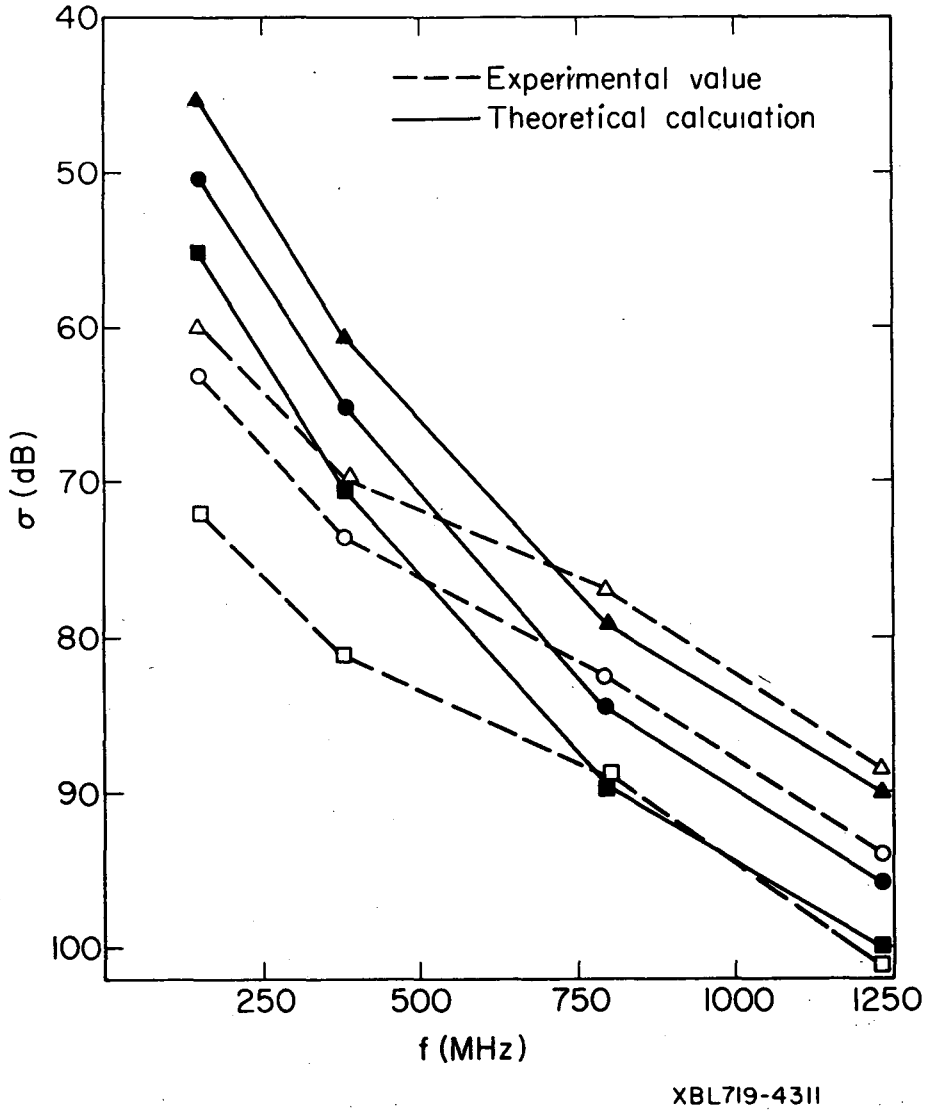
Experimental value
Theoretical calcuiation
σ (dB)
f (MHz)
40
50
60
70
80
90
100
250
500
750
1000
1250
XBL719-4311

Fig. 10.

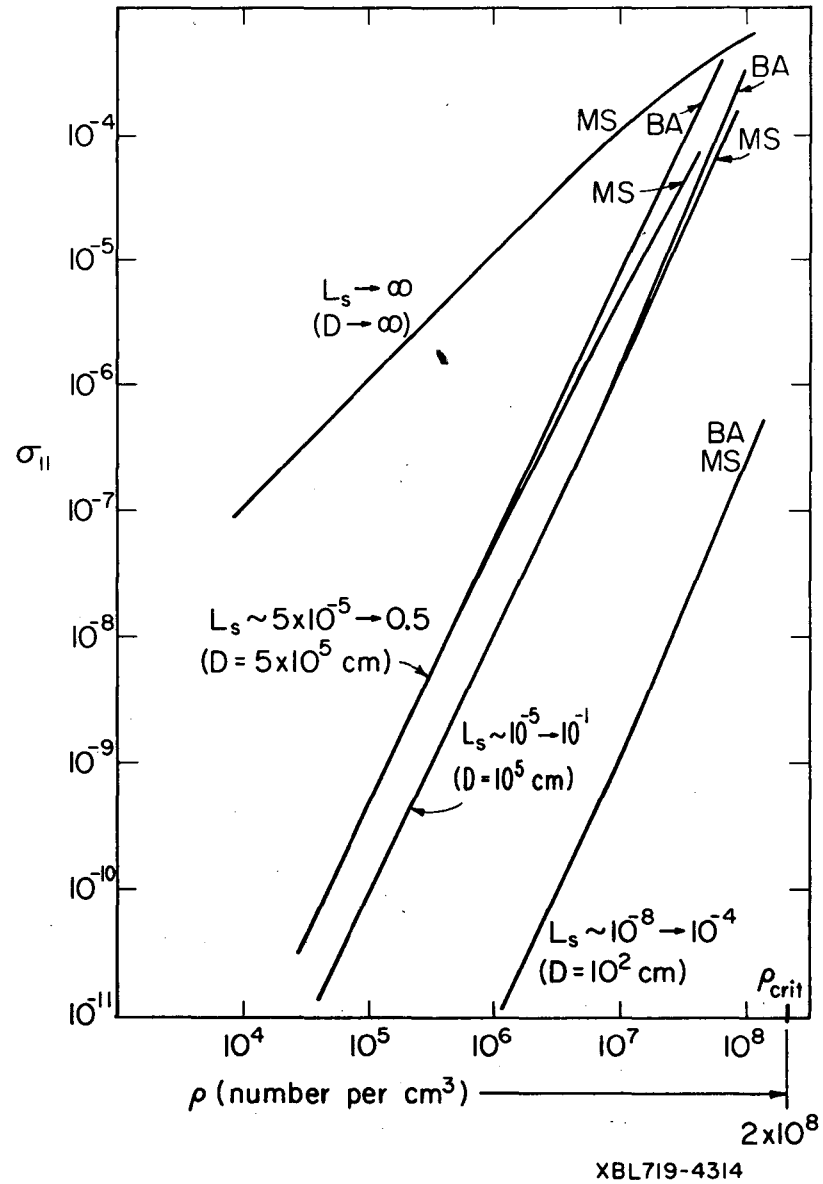
BA
MS
BA
MS
MS
$L_s \to \infty$
$(D \to \infty)$
BA
MS
$L_s \sim 5\times10^{-5} \to 0.5$
$(D = 5\times10^5$ cm)
$L_s \sim 10^{-5} \to 10^{-1}$
$(D = 10^5$ cm)
$L_s \sim 10^{-8} \to 10^{-4}$
$(D = 10^2$ cm)
ρ_{crit}
$\sigma_{\perp}$
10^{-4}
10^{-5}
10^{-6}
10^{-7}
10^{-8}
10^{-9}
10^{-10}
10^{-11}
10^4
10^5
10^6
10^7
10^8
ρ (number per cm^3)
2×10^8
XBL719-4314

Fig. 11.

TECHNICAL INFORMATION DIVISION
LAWRENCE BERKELEY LABORATORY
UNIVERSITY OF CALIFORNIA
BERKELEY, CALIFORNIA 94720